Journal of Molecular and Cellular Cardiology 79 (2015) 54–68

Contents lists available at ScienceDirect

Journal of Molecular and Cellular Cardiology

journal homepage: www.elsevier.com/locate/yjmcc

Original article

Redox regulation of cardiomyocyte cell cycling *via* an ERK1/2 and c-Myc-dependent activation of cyclin D2 transcription

Thomas V.A. Murray, Ioannis Smyrnias, Moritz Schnelle, Rajesh K. Mistry, Min Zhang, Matteo Beretta, Daniel Martin, Narayana Anilkumar, Shana M. de Silva, Ajay M. Shah, Alison C. Brewer *

King's College London British Heart Foundation Centre of Research Excellence, Cardiovascular Division, London, UK

ARTICLE INFO

Article history:
Received 18 July 2014
Received in revised form 22 October 2014
Accepted 24 October 2014
Available online 6 November 2014

Keywords:
Cardiomyocyte proliferation
ERK1/2
Nox4
Cyclin D2
Redox signalling
c-Myc

ABSTRACT

Adult mammalian cardiomyocytes have a very limited capacity to proliferate, and consequently the loss of cells after cardiac stress promotes heart failure. Recent evidence suggests that administration of hydrogen peroxide (H_2O_2), can regulate redox-dependent signalling pathway(s) to promote cardiomyocyte proliferation *in vitro*, but the potential relevance of such a pathway *in vivo* has not been tested. We have generated a transgenic (Tg) mouse model in which the H_2O_2-generating enzyme, NADPH oxidase 4 (Nox4), is overexpressed within the postnatal cardiomyocytes, and observed that the hearts of 1–3 week old Tg mice pups are larger in comparison to wild type (Wt) littermate controls. We demonstrate that the cardiomyocytes of Tg mouse pups have increased cell cycling capacity *in vivo* as determined by incorporation of 5-bromo-2′-deoxyuridine. Further, microarray analyses of the transcriptome of these Tg mouse hearts suggested that the expression of cyclin D2 is significantly increased. We investigated the molecular mechanisms which underlie this more proliferative phenotype in isolated neonatal rat cardiomyocytes (NRCs) *in vitro*, and demonstrate that Nox4 overexpression mediates an H_2O_2-dependent activation of the ERK1/2 signalling pathway, which in turn phosphorylates and activates the transcription factor c-myc. This results in a significant increase in cyclin D2 expression, which we show to be mediated, at least in part, by *cis*-acting c-myc binding sites within the proximal cyclin D2 promoter. Overexpression of Nox4 in NRCs results in an increase in their proliferative capacity that is ablated by the silencing of cyclin D2. We further demonstrate activation of the ERK1/2 signalling pathway, increased phosphorylation of c-myc and significantly increased expression of cyclin D2 protein in the Nox4 Tg hearts. We suggest that this pathway acts to maintain the proliferative capacity of cardiomyocytes in Nox4 Tg pups *in vivo* and so delays their exit from the cell cycle after birth.

1. Introduction

Unlike many other organs, the adult mammalian heart has a very limited capacity to regenerate after injury. Adult cardiomyocytes are essentially post-mitotic and do not re-enter the cell cycle in sufficient numbers to achieve efficient repair, for example after an ischemic insult (reviewed in [1]). However the foetal mouse heart can restore homeostasis after injury by increased proliferation of existing cardiomyocytes [2], and this ability is transiently maintained in the postnatal mouse heart [3]. By 7 days of age this regenerative capacity is lost, as the cardiomyocytes terminally exit the cell cycle [1,4].

Understanding the mechanisms underlying the cell-cycle arrest in postnatal cardiomyocytes is therefore of paramount importance to inform future therapeutic strategies to increase the regenerative potential of the injured adult heart. There is now much evidence to suggest that the proliferation of many cell types is under the control of redox-regulated signalling pathways (reviewed in [5]). In particular the ERK1/2 signalling cascade, activated by intracellular-generated reactive oxygen species (ROS) acts to promote proliferation in various cell types [6–8]. An important molecular mechanism underlying this ERK1/2 activation is thought to be the ROS-dependent inactivation of protein tyrosine phosphatases (PTPs) (reviewed in [9]). However, very little is known of the molecular pathways which transduce ERK1/2 activation to cell proliferation. In cardiac cells, treatment of neonatal mouse cardiomyocytes *in vitro* with a low level of the ROS hydrogen peroxide (H_2O_2) was shown to stimulate proliferation by approximately 30% [10]. Further, in a separate study of cardiomyocytes differentiated from murine ES cells, cardiotrophin-induced proliferation was shown to involve the redox activation of ERK1/2 [11]. Recently, ERK1/2 activation was also shown to be associated with increased cytokine-induced proliferation of the cardiac cell line, HL-1 [12].

It is now evident that the family of NADPH oxidase proteins (Noxs) is an important enzymatic generator of intracellular ROS which modulate

Abbreviations: BrdU, bromodeoxyuridine; AdNox4, adenoviral Nox4; AdβGal, adenoviral β-galactosidase; PEG, polyethylene glycol; Wt, wild type; Tg, transgenic; NRC, neonatal rat cardiomyocyte.

* Corresponding author. Tel.: +44 207 848 5340; fax: +44 207 848 5193.
E-mail address: alison.brewer@kcl.ac.uk (A.C. Brewer).

http://dx.doi.org/10.1016/j.yjmcc.2014.10.017

redox-sensitive signalling pathways [13]. There are 7 Nox isoforms that have been identified in mammalian species (Nox1–5 and Duox1/2) which show specificity of cellular distribution, intracellular location, mechanisms of action and types of ROS produced [14]. Many studies have demonstrated that NADPH oxidases are involved in the regulation of cell proliferation *via* redox-mediated cell signalling pathways *in vitro*, and the involvement of ERK1/2 has been shown in many cases (reviewed in [15]). However, the significance of these observations with respect to cardiomyocytes has not, thus far, been tested *in vivo*. Various Nox isoforms are widely expressed in all cardiovascular cells, and we and others have demonstrated previously that Nox2 and Nox-4 are co-expressed in cardiomyocytes [16–18]. Of particular interest is the observation that the expression of endogenous Nox4 within the heart declines sharply over the period of birth [16]. Furthermore, by contrast to Nox2 which generates the superoxide anion (O_2^-), Nox4 has been shown to produce predominantly H_2O_2 [19,20] which is the specific type of ROS demonstrated to enhance cardiomyocyte proliferation [10]. Thus, potentially, a decreased level of intracellular Nox4-generated ROS and consequent downstream signalling within cardiomyocytes after birth may contribute to their decline in proliferative potential *in vivo*.

Many studies have aimed at determining important regulatory molecules that control proliferation of the cardiomyocyte, and its exit from the cell cycle (reviewed in [21]). The cardiac expression levels of many of the known mammalian cell cycle regulators such as cyclins, cyclin-dependent kinases (Cdks) and Cdk inhibitors have been determined over the periods of embryonic, perinatal and adult development. As might be expected, positive cell cycle regulators (such as the cyclins and Cdks) become downregulated as the cardiomyocytes exit the cell cycle, while negative regulators (such as the Cdk inhibitors) frequently are upregulated in post-mitotic cardiac cells [21]. Of particular note are the D-type cyclins (cyclins D1, D2 and D3), which are all highly expressed in the embryonic heart and become progressively downregulated in the neonatal and adult cardiomyocytes. Ablation of all three D-type cyclins in embryonic mice leads to cardiac abnormalities and death [22]. By contrast, cardiac-specific transgenic overexpression of cyclin D1, D2 or D3 has been shown, *per se*, to promote DNA synthesis within adult cardiomyocytes [23], and recently cyclin D2 overexpression was demonstrated to be sufficient to enhance overt cardiomyocyte proliferation in the postnatal heart [24].

We demonstrate here that cardiomyocyte-specific overexpression of Nox4 in a Tg mouse model results in an increase in the proliferative capacity of the cardiomyocytes in the postnatal heart, and that this correlates with a significant increase in cyclin D2 expression. We have therefore investigated *in vitro* the ROS-dependent molecular mechanisms which underlie this increase in cardiomyocyte-cycling and identify an ERK1/2-dependent pathway that results in cyclin D2 upregulation *via* the activation of the protooncogene, c-myc. Thus mediators of this pathway, linking intracellular ROS to increased cyclin D2 expression may be promising therapeutic targets to help promote cardiomyocyte proliferation after cardiac injury.

2. Materials and methods

2.1. Genetically-modified mice and experimental animals

Cardiomyocyte-targeted Nox4-transgenic (Nox4 Tg) mice have been described previously [16]. Neonatal Sprague–Dawley rats (born within 24 h) were purchased from Harlan Laboratories UK.

2.2. Cell culture

Neonatal rat cardiomyocytes (NRCs) were isolated and cultured as previously described [16]. Where indicated, NRCs were treated with either 20 μM PD98059 (Sigma, MEK1 inhibitor) or DMSO (0.1%) as vehicle control. For catalase treatments, 400 U/ml of PEG-conjugated catalase (Sigma) was added overnight. Nuclear extracts were prepared as previously described [25].

2.3. Bromodeoxyuridine labelling and ELISA

Bromodeoxyuridine (BrdU) was used to label cycling cells *in vivo*. Experimental mice were injected intraperitoneally with BrdU (167 mg/kg; Sigma) and sacrificed after 16 h, when the heart tissue was isolated. DNA samples were purified, and coated overnight in triplicate onto 96 well plates, previously treated with poly L-lysine (0.01% in PBS), at a final concentration of 100 μg/ml in 1× SSC (150 mM sodium chloride, 15 mM sodium citrate) after boiling (5 min). Wells were blocked with 3% BSA, 1.5% normal goat serum for 1 h and subsequently incubated for 2 h with 1:100 dilution of BrdU antibody (Abcam). After washing with PBS, antibody binding was assessed using the peroxidase-based immunodetection kit (Vectastain Elite ABC kit, Vector Laboratories) and the 1-step ABTS solution (Thermo Scientific). Absorbance was measured at 405 nm.

2.4. Construction of mouse cyclin D2 luciferase reporter plasmid and luciferase reporter assays

The cyclin D2 luciferase reporter plasmid was constructed by inserting a 1766 bp PCR-amplified fragment of the cyclin D2 promoter (−15 bp to −1781 bp relative to the start of translation) between the Kpn1 and Xho1 sites of pGL4.22[luc2CP/Puro] luciferase vector (Promega) by standard techniques. The mouse cyclin D2 promoter fragment was generated with the primer pair 5′- GGAATGGTACCCGCCCCAAACTCATACTCAC -3′ (incorporating a 5′ Kpn1 restriction site) and 5′- GGAATCTCGAGACTCG GTCCCGACTGTAAATT -3′ (incorporating a 3′ Xho1 restriction site), using Herculase (Stratagene) and mouse genomic DNA as template. The fidelity of the plasmid construct was confirmed by sequencing. Alignment of the mouse and human cyclin D2 promoter sequences was performed using Clustal W software [26]. Luciferase reporter assays were performed as previously described [27].

2.5. Viral transductions and siRNA-mediated knockdown in NRCs

Full-length mouse cDNA of Nox4 was obtained as a kind gift from Thomas Leto. Adenoviral expression vectors were generated for Nox4 (AdNox4) and β-galactosidase (AdβGal) as described previously [27]. Cells were transduced with adenoviral constructs at a multiplicity of infection (MOI) of 20 and incubated overnight prior to use. For siRNA studies, siRNA targeted against rat cyclin D2, rat c-myc or scrambled control (Ambion) was transfected into NRCs at a concentration of 5 nM using Lipofectamine2000™ reagent according to the manufacturer's protocol.

2.6. Western blotting

Cells or tissue samples were homogenised and proteins were separated for immunoblot analysis as previously described [27]. Nuclear extracts were prepared using the NE-PER nuclear protein extraction kit (Thermo-Fisher) as per the manufacturer's instructions. Primary antibodies and the dilutions that were used were as follows: phospho-p44/p42 MAPK (ERK1/2 Thr202/Tyr204), p44/p42 MAPK (total ERK1/2), cyclin D1, Cdc2, Cdc6 and Cdk4 (Cell Signaling Technology; all used at a dilution of 1:1000); and cyclin D2, cyclin A2 (Abcam, 1:1000), lamin A/C (Santa Cruz, 1:2000), total c-myc (1:1000, cell signalling), phosphor-c-myc (Thr58/Ser62) (1:1000, Millipore) α-tubulin (1:4000) and β-actin (1:5000, Sigma).

2.7. Cardiomyocyte isolation and volume measurements

Excised hearts were fixed in 4% PFA for 4 h, washed with PBS and subsequently digested with collagenases B and D (Roche: 1.8 mg/ml

and 2.4 mg/ml respectively) at 37 °C as necessary until individual cardiomyocytes became dissociated. Isolated cardiomyocytes were washed and stored in PBS. Cardiomyocyte volumes were then assessed in a Multisizer-3 Coulter Counter (Beckman). For assessment of BrdU incorporation, aliquots of cells were spun onto poly-L-lysine-treated slides (1000 rpm, 3 min), in a Shandon Cytospin 4. Immobilised cells were permeabilised (0.5% triton, 15 min) and then treated with 50 units/ml RQ1 DNAse1 (Promega) at room temperature for 45 min before immunostaining. For assessments of cell volume based on physical cell measurements, mouse ventricular myocytes were isolated by Langendorff perfusion and enzymatic dispersion. Mice were anaesthetized by intraperitoneal injection of sodium pentobarbitone (60 mg/kg) and heparin (100 IU). Hearts were excised, transferred to ice cold perfusion buffer [(mM): NaCl, 140; KCl, 5; NaH_2PO_4, 2; $CaCl_2$, 1.36; $MgSO_4$, 1.2; glucose, 10; HEPES, 5; Taurine, 20; creatine, 10; pH 7.3–7.4]. After cannulation, hearts were mounted on Langendorff apparatus and perfused with pre-warmed, oxygenated perfusion buffer, before calcium depletion using EGTA (100 mM) containing buffer for 5 min and finally perfused with 0.5 mg/ml collagenase (type 2, activity 285 U/ml, Worthington Biomedicals, Lakewood, NJ, USA) for 13 min. Ventricular tissue was removed, dispersed, triturated gently and filtered through a 200 μm nylon mesh before graded calcium reintroduction. The cell suspension was allowed to stabilize at room temperature for 30 min and then fixed in 4% PFA (final) for 2 h at 4 °C. Myocytes were measured along their long axis to determine cell lengths and along the cross section at their midpoint to determine cell width. On average, approximately 100 cells were analysed per condition from three different preparations. Cell volume was calculated as previously described [28].

2.8. Echocardiography

Mice were anaesthetised with 1.5% isoflurane and imaged using a Vevo 2100 Imaging System with a 40-MHz linear probe (Visualsonics, Canada). Systolic function, septal and posterior wall thickness and left ventricular diameter were assessed using M-mode imaging in both short and long axis views. The relative wall thickness (RWT) in diastole for each heart was calculated as follows: RWT = (septal wall thickness + posterior wall thickness) / left ventricular diameter.

2.9. cDNA synthesis and Q-PCR

Total RNA extraction, cDNA syntheses and Q-PCR analyses were performed as described previously [29]. Forward (F) and reverse (R) primers used to detect rat and mouse transcripts were as follows (all 5′-3′): rat β-actin; F: *CCCGCGAGTACAACCTTCT,* R: *CGTCATCCATGGCG AACT;* rat cyclin D2; F: *CACCGACAACTCTGTGAAGC*, R: *CCACTTCAGCTTAC CCAACAC;* mouse β-actin; F: *CTGTCGAGTCGCGTCCACCC*, R: *ATGCCGGAGC CGTTGTCGAC;* mouse Nox4; F: *CCGGACAGTCCTGGCTTATC,* R: *TGCTTTTA TCCAACAATCTTCT;* mouse cyclin D2; F: *TCCCGTTGAGTGGGGCAAGGT,* R: *ACCCGAGACCACAGAAACAGCCT;* mouse cdc2; F: *GATACGAGTGTACACACA CGA,* R: *AACCGGAGTGGAGTAACGAG;* mouse cdk4; F: *TCAGTGGTGCCAGA GATGG,* R: *GGAAGGCAGAGATTCGCTTA;* mouse cyclin A2; F: *CAGCATGA GGGCCATCCTT,* R: *GCAGGGTCTCATTCTGTAGTTTA;* mouse cyclin D1; F: *AGCCAGCTGCAGTGCTGTAC,* R: *CTGGTGGTGCCCGTTTTG;* mouse cdc6; F: *GAAATTGTGGAGTCGGATGTCA,* R: *CGACTCGCTGGGTGATTTACA;* rat c-myc F: *GAATTTTTGTCTATTTGGGGACA;* R: *GCATCGTCGTGACTGTCG.*

2.10. Immunocytochemistry and histochemistry

Immunocytochemistry and histochemistry were performed on 6-μm sections cut from paraffin-embedded Wt or Tg hearts (including those isolated from mice that had been injected with BrdU as described above) or 8 μm sections cut from cryopreserved Wt or Tg heart tissue. All sections were fixed in 3.3% paraformaldehyde, and permeabilised with 0.1% triton X-100 in PBS. FITC-conjugated wheat germ agglutinin (WGA) was used to outline cardiomyocytes as described previously [16]. For BrdU staining, sections were initially treated with 1 N HCl (10 min on ice), 2 N HCl (10 min at room temperature, then 20 min at 37 °C) and washed twice with borate buffer to facilitate antigen exposure to the antibody. Primary antibodies against laminin (Sigma), Ki67 (Vector Laboratories), cardiac troponin T (Abcam) and BrdU (Abcam) were used at dilutions of 1:250, 1:200, 1:500 and 1:100 respectively. For laminin staining, antibody binding was assessed using the peroxidase-based Vectstain Elite ABC kit and diaminobenzidine (ImmPACT DAB; both Vector Laboratories). All other antibody bindings were visualised using Alexa 568-conjugated anti-mouse IgG and 488-conjugated anti-rabbit IgG secondary antibodies (Invitrogen Molecular Probes; 1:200 dilution). Rat neonatal cardiomyocytes were cultured on cover slips, before fixation, permeabilisation and staining as above. Images were visualised using a Nikon Axioscope microscope with Openlab software (Improvision), an Olympus inverted fluorescence microscope with Velocity software (PERKinElmer), or a Leica scanning confocal microscope (TCS-SP5). Red and green fluorescent signals were detected using appropriate filter sets (excitation 568/emission 620 nm or 488/emission 505–530 nm respectively). Confocal images were acquired as transcellular 0.4 μm sections in the Z plane (15 scans/plane).

2.11. Cell proliferation assays

NRCs were seeded (1.5×10^4 cells/well) on a 96-well cell culture plate that had been coated with a 1% gelatin solution. Cells were transduced with an adenovirus vector encoding either Nox4 (AdNox4) or β-galactosidase (AdβGal) as control at an MOI of 20. Cells were incubated for 24 h and cell proliferation was assessed by colorimetric MTS assay (CellTiter 96® AQueous One Solution Cell Proliferation Assay, Promega) as per manufacturer's instructions. Manual cell counts were performed using a haemocytometer. Cells were seeded at a density of 2.5×10^5 cells/well in a 6-well cell culture plate and transduced with virus as outlined above. After incubation cells were harvested by treatment with trypsin–EDTA until a single cell solution was obtained and counted. 6 repeats of each condition were performed.

2.12. Flow cytometry and cell cycle analysis

NRC cells were treated as indicated. A single cell suspension of cells was obtained by trypsinisation and the cells were fixed in 70% methanol overnight. Cells were stained with propidium iodide (50 μg/ml dissolved in PBS containing 5 U/ml RNase A) and were analysed using a FACScalibur flow cytometer (BD Biosciences) using appropriate doublet discrimination. A minimum of 10,000 cells were analysed per sample. Cell cycle data were generated using ModFit LT version 4.0.

2.13. Statistics

Data are expressed as mean ± SEM. Comparisons between sample groups or measurements at different time points were made by unpaired two-tailed Student's *t*-test. Heart/body weight ratios of 5 and 7 week-old Wt and Tg mice were additionally analysed by one-way ANOVA with Bonferroni post-hoc test, as indicated.

3. Results

3.1. Forced postnatal expression of Nox4 in cardiomyocytes in vivo results in overt cardiac enlargement in mouse pups

We have described previously a Nox4 cardiac-specific overexpressing transgenic (Tg) mouse in which the expression of Nox4 is under the control of the alpha myosin heavy chain (αMHC) promoter [16,29]. Consistent with the endogenous developmental pattern of expression of αMHC, Nox4 mRNA and protein expression are strongly upregulated, specifically within the myocardium, from birth in this mouse

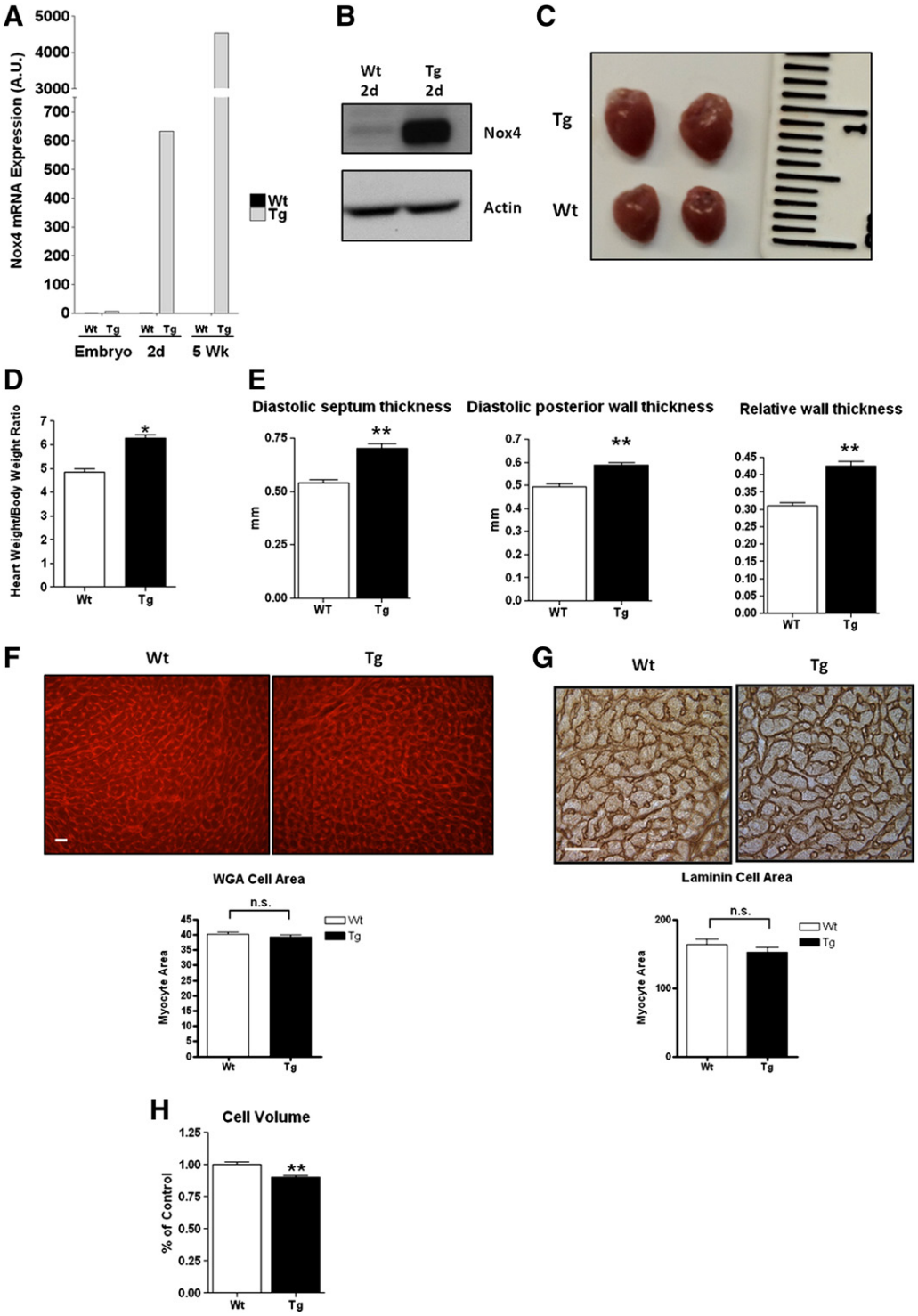

Fig. 1. Forced postnatal expression of Nox4 in cardiomyocytes *in vivo* results in overt cardiac hypertrophy. (A) Q-PCR analysis of Nox4 mRNA expression in Tg and Wt littermate control mouse hearts at embryonic day 18 and 2 days and 7 weeks post-birth. Expression levels are normalised to those of β-actin and as expressed as arbitrary units relative to endogenous Nox4 expression within the embryo (A.U.). (B) Nox4 protein levels in 2 day postnatal Wt and Tg hearts. (C) Representative picture depicting the proportional increase in the size of hearts isolated from 2 week old Wt and Tg mice. (D) Quantification of heart/body weight ratios of Wt ($n = 15$) and Tg ($n = 12$) mice. (E) Echocardiographic measurements of interventricular septum thickness, left ventricular posterior wall thickness and relative wall thickness in 3 week old Wt ($n = 5$) and Tg ($n = 7$) mice taken at the end of diastole. (F & G) Representative transverse heart sections for cardiomyocyte area determination from Wt and Tg mice stained with either WGA (F) or an antibody against laminin (G). Mean data are shown in a histogram beneath each stained section. Scale bar, 10 μm. (H) Comparison of isolated cardiomyocyte cell volumes from 2 week old Wt and Tg animals, assessed on a Coulter Counter. All data are presented as mean ± S.E. $^{*}P < 0.05$, $^{**}P < 0.01$.

(Figs. 1A, B), while endogenous levels of Nox4 are not significantly affected (Supplementary data, Fig. S1A). We reported that under normal physiological conditions, the hearts of the adult Nox4-overexpressing mice are phenotypically similar to those of wild type (Wt) littermate controls both in size and cardiac function [16]. However, at two weeks of age we found that the Nox4 Tg mouse hearts were overtly enlarged and exhibited a significant, approximately 30% increase in heart weight/body weight ratio when compared to Wt littermate controls

(4.85 ± 0.12 *vs.* 6.28 ± 0.13; Figs. 1C & D). Echocardiographic measurements confirmed that there were significant increases in both the left ventricular posterior wall thickness and the interventricular septal wall thickness at diastole in 3 week-old Tg mouse hearts when compared with littermate Wt controls (Fig. 1E). Further, the relative left ventricular wall thickness (RWT) was increased in the Tg mouse hearts, consistent with concentric rather than eccentric hypertrophic growth (Fig. 1E). Despite this hypertrophy the contractile function, as determined by ejection fraction, was preserved in these Tg mice (Supplementary data, Fig. S1B). To show that the increase in heart size was not due to potential positional effects of transgene insertion, the heart weight/body weight ratios were also determined in a second, distinct, cardiac-specific Nox4 Tg mouse line. A significant difference in heart weight/body weight was similarly evident in this line (4.80 ± 0.18 *vs.* 5.60 ± 0.23; Supplementary data, Fig. S1C), confirming that this phenotype is indeed a result of Nox4 overexpression.

We initially investigated whether the increase in heart size could be explained by increased cardiomyocyte size (cellular hypertrophy). Transverse sections of Wt and Tg 2-week-old mouse hearts were stained to determine the average cross-sectional cardiomyocyte area of the two groups. As shown in Figs. 1G and H, no increase in the cross-sectional area of the cardiomyocytes was observed, as assayed by histological staining with wheat germ agglutinin (WGA; Fig. 1F), or by immunological staining with an antibody to laminin (Fig. 1G). Further, we measured the cellular volume of cardiomyocytes isolated from the 2 groups, and found a small but significant decrease in the average size of the Tg cardiomyocytes (Fig. 1H). Thus the increase in heart size in the Tg mice could not be explained by an increase in cardiomyocyte size.

3.2. Nox4 Tg hearts demonstrate increased cardiomyocyte cell cycling

To assess whether increased cellular proliferation and cardiomyocyte cell number account for the increased heart/body weight ratio in Tg mouse hearts, the nucleotide analogue bromo-deoxyuridine (BrdU) was injected into 2-week-old Tg and Wt littermate mice, 16 h before they were sacrificed. To obtain a quantitative measure of BrdU incorporation in Wt and Tg hearts, an ELISA assay for BrdU incorporation was performed and showed an approximate 38% increase in BrdU incorporation in Tg hearts when compared to Wt controls (2.27 ± 0.22 A.U. *vs.* 3.13 ± 0.32 A.U.; Fig. 2A). Consistent with this observation, sections from Wt and Tg hearts co-stained with DAPI and an anti-BrdU antibody revealed that the proportion of BrdU-positive, and therefore actively cycling cells was markedly higher in Tg heart sections, compared to Wt controls (Fig. 2B). A significant proportion of these BrdU-positive nuclei has a distinctive morphology characteristic of longitudinal sectioning through cardiomyocyte nuclei (white arrows in Fig. 2C). To definitively demonstrate increased cycling of cardiomyocytes in this mouse model, cardiomyocytes were isolated from (BrdU-injected) 2 week old Wt and Tg hearts and co-stained with antibodies to cardiac α-actinin T (red) and BrDU (green) (Figs. 2D & E). The proportion of cycling cardiomyocyte nuclei was found to be significantly greater in the Tg group (7.00% ± 0.84%, *vs.* 1.87% ± 0.41%; $P < 0.001$). Similar results were obtained in heart sections stained with the cell cycle marker, Ki67 (see Supplementary data, Figs. S2A–C). Thus cardiomyocyte-specific overexpression of Nox4 *in vivo* resulted in a cell-autonomous increase in cell-cycling activity which would explain the increased heart size that we observed.

3.3. Nox4 Tg hearts display increased levels of expression of specific cell-cycle regulating genes, and in particular cyclin D2

Cellular proliferation is tightly controlled by members of the cyclin and cyclin-dependent kinase (Cdk) family of proteins (reviewed in [4]). Upon analysis of a microarray study comparing the transcriptomes of 2-week old Nox4 Tg and Wt hearts that we have previously performed [29], we observed a striking transcriptional upregulation of cyclin D2 expression in the Tg hearts. This was the only cyclin or Cdk family member to show such a significant (greater than 2-fold) increase in this array. Cyclin D2 is known to be both necessary and sufficient for cardiomyocyte cell cycling *in vivo*. Thus cell cycle re-entry is completely blocked in the myocardium of cyclin D2-deficient hearts [30] while the forced expression of cyclin D2 alone has previously been demonstrated to be sufficient to increase the cell cycling capacity of cardiomyocytes both *in vitro* and *in vivo* [24,31,32]. The expression of cyclin D2 protein is high in the embryonic heart, but drops dramatically after birth to very low levels in the normal postnatal heart by 2 weeks of age (Fig. 3A), concomitant with cardiomyocyte cell cycle exit. Q-PCR confirmed that cyclin D2 mRNA was significantly increased in hearts from two week old Tg compared to Wt animals (Fig. 3B), and cyclin D2 protein levels were also shown by immunoblot to be significantly increased in these Tg hearts (Fig. 3C).

More modest increases in mRNA levels of the cell-cycle-regulating proteins, cyclin A2, cdc2 and cdk4 were also in our microarray screen [29]. To further characterise the molecular mechanisms underlying the increased cardiomyocyte cell cycling in this mouse model we therefore determined the mRNA and protein levels of these genes, in the 2 week Wt and Tg mouse hearts. We additionally investigated the expression levels of cell division cycle 6 (cdc6), which was not found to be increased at the level of mRNA in our microarray, but which is known to be absolutely required for entry into S phase [33]. In broad agreement with our microarray data, the mRNA expression levels of cdc2 and cyclin A2 were found to be increased in Tg, compared to Wt hearts (Fig. 3D), while at the protein level, we also observed a significant increase in cdc2, but not cyclin A2 (Fig. 3E). In the case of cdc6, in agreement with our microarray data, we found no difference in the mRNA levels between Tg and Wt hearts but we did observe a striking increase in cdc6 protein levels, suggesting a post-transcriptional level of regulation (Figs. 3D & E). For cdk4, we did not demonstrate a significant difference in mRNA or protein expression between Tg and Wt mouse hearts (Figs. 3D & E).

3.4. Nox4 acts as an enzymatic source of ROS to promote proliferation of neonatal cardiomyocytes via an ERK1/2-dependent mechanism

In order to investigate the molecular mechanisms underlying the increased cardiomyocyte-cycling seen in the Nox4 Tg hearts, we overexpressed Nox4 in isolated neonatal rat cardiomyocytes (NRCs). NRCs were transduced with an adenoviral vector containing either a Nox4 (AdNox4) or β-galactosidase (AdβGal) transgene for 24 h and cardiomyocyte proliferation was assessed both by an MTS-based cell proliferation assay and by physical counting of cardiomyocyte cell number. As shown in Fig. 4A, Nox4 transduction increased Nox4 protein expression and furthermore induced a significant increase in cardiomyocyte proliferation, as assessed by the MTS-based assay (100 ± 8.38% *vs.* 127.96 ± 7.31%; Fig. 4B), and confirmed by cell counting (Fig. 4C). In addition, FACS analyses revealed that this enhancement of cell proliferation correlated with a significant decrease (approximately 5%) in the percentage of cells in the G_0/G_1 phase of the cell cycle and a corresponding increase in the proportion of cells present in the G_2/M phase of the cell cycle upon Nox4 overexpression (Fig. 4D). The proportion of cell in S phase remained unchanged between the two groups.

We have shown previously that Nox4 activates ERK1/2 in HEK293 cells [34]. ERK1/2 is known to be a critical regulator of the cell cycle and to promote and/or associate with increased proliferation in various cell types [35], including NRCs [12]. In NRCs, overexpression of Nox4 significantly increased ERK1/2 phosphorylation. Inhibition of MEK1 (an upstream activator of ERK1/2) by the addition of PD98059, inhibited both the basal level of ERK1/2 activation, and the increased phosphorylation seen upon Nox4 overexpression (Fig. 4E). In addition, the Nox4-dependent activation of ERK1/2 was demonstrated to be ROS-dependent, as it was ablated by the addition of PEG-catalase (Fig. 4F).

We assessed the effect of the inhibition of ERK1/2 activation upon cardiomyocyte cell cycling, and found that the presence of PD98059

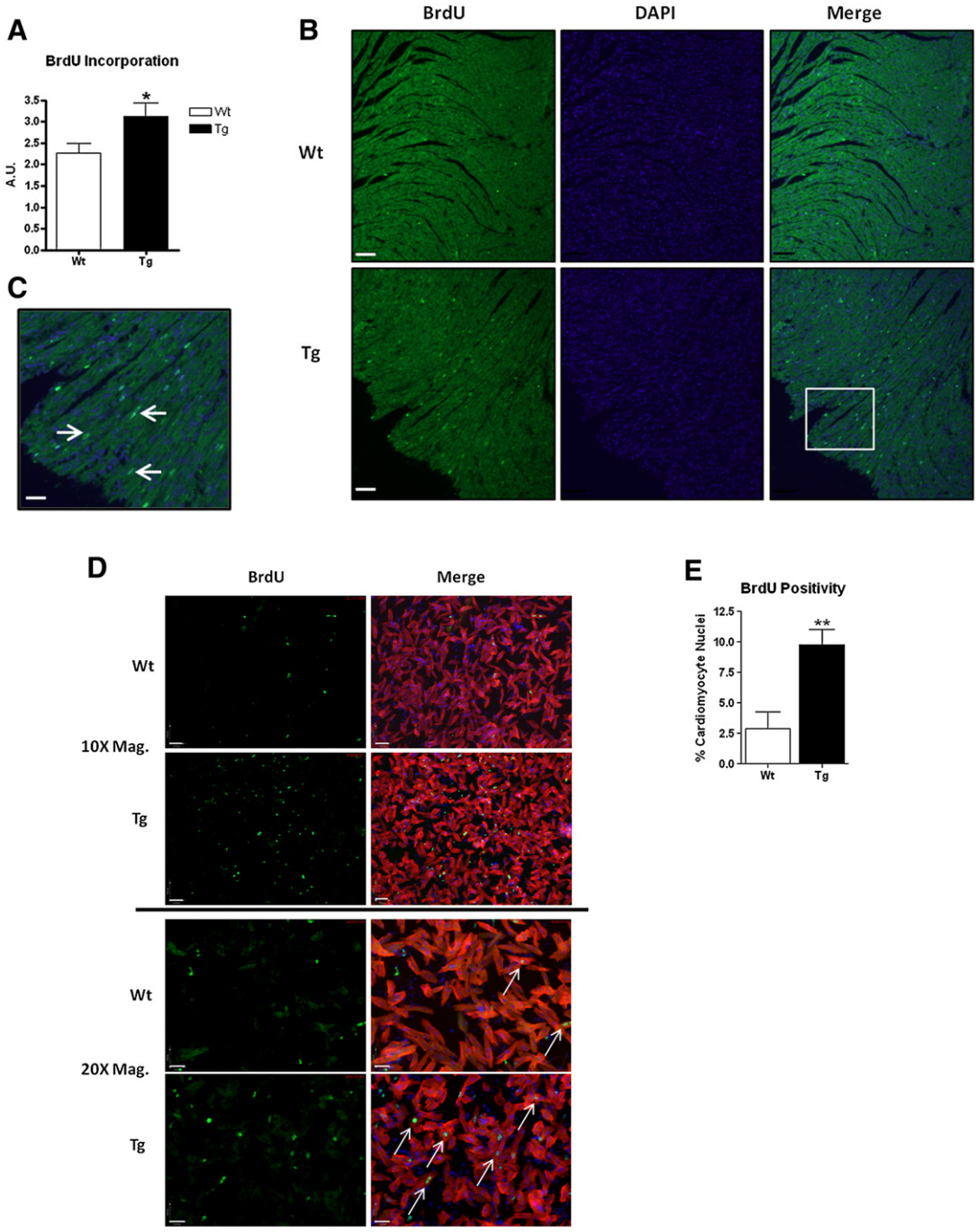

Fig. 2. Nox4 transgenic hearts demonstrated increased cardiomyocyte cell cycling. (A) ELISA assay of BrdU incorporation from hearts isolated from BrdU injected 2 week old Wt and Tg pups. Pups were injected with BrdU and sacrificed after 16 h. (B) Representative immunofluorescence staining of transverse sections of equivalent paraffin-embedded hearts from BrDU-injected Wt and Tg mouse pups. BrdU-labelled, DNA-synthesising nuclei (green) and DAPI-stained nuclei (blue) are visible. Scale bar, 60 μm. (C) Magnified section from Tg heart section above (white box) depicting BrdU-labelled nuclei. Elongated nuclei consistent with cardiomyocyte morphology are indicated by white arrows. Scale bar, 25 μm. (D) Cardiomyocytes isolated from equivalent BrDU-injected Wt and Tg hearts were co-stained with antibodies against BrdU (green) and cardiac troponin T (red) and the cell nuclei stain DAPI (blue). Representative images are shown at low magnification (10×; scale bar, 110 μm) and at higher magnification (20×; scale bar, 54 mm). (D) Quantitation of percentage of BrdU-stained cardiomyocyte nuclei/field of view (n = 13 & 7 fields of view, each comprising approx. 200 cardiomyocyte nuclei). All data are presented as mean ± S.E. $^{*}P < 0.05$.

also ablated the observed Nox4-dependent increase in proliferation (Fig. 4G). In addition, the decrease in the proportion of cells in the G_1/G_0 phase of the cell cycle and the increase in the proportion of cells in G_2/M, that were apparent upon Nox4 overexpression, were ablated by ERK1/2 inhibition (Fig. 4H). Thus Nox4-derived ROS acts, at least in part, *via* a MEK1-dependent mechanism to activate ERK1/2 and consequently promote proliferation in neonatal cardiomyocytes. Additionally, consistent with our *in vitro* observations, ERK1/2 phosphorylation was significantly increased in Tg hearts when compared with Wt littermate control hearts (Fig. 4I).

3.5. Nox4-induced proliferation is mediated by the upregulation of cyclin D2

Consistent with our *in vivo* data, isolated NRCs transduced with AdNox4 showed both an increase in cyclin D2 mRNA expression

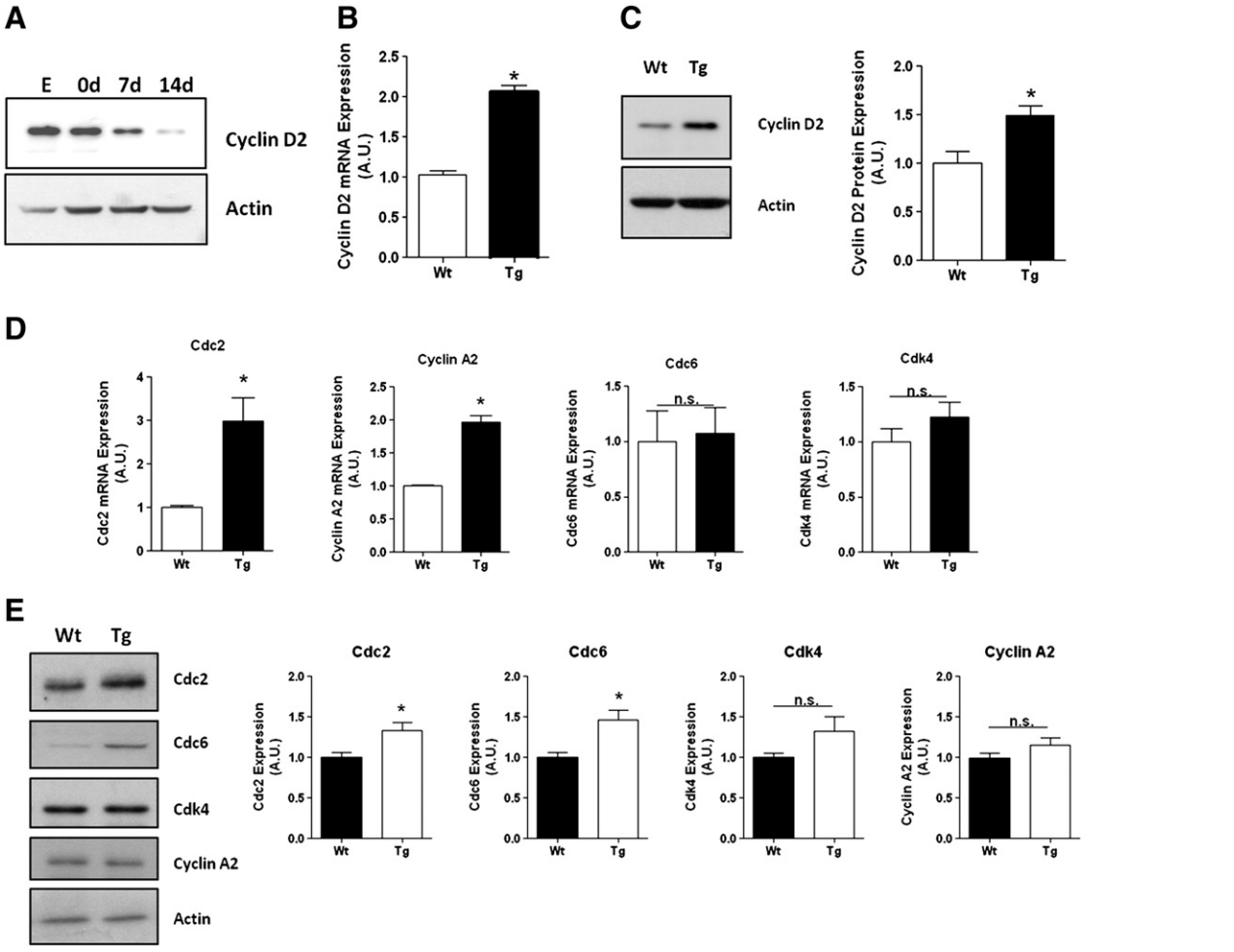

Fig. 3. Nox4 overexpression induces the upregulation of cyclin D2 *in vivo*. (A) Expression levels of cyclin D2 protein during development from Wt mice at embryonic day 14.5, birth (day 0), and 7 days and 14 days postnatal. (B) Q-PCR analysis of the relative expression of endogenous cyclin D2 mRNA in 2 week old Wt and Tg mouse hearts. Triplicate, independent Tg and Wt littermate controls were analysed, and relative expression was normalised to β-actin in all cases. (C) Protein expression levels of cyclin D2 in Wt and Tg hearts at 2 weeks of age. The histogram depicts the mean of triplicate, independent samples normalised to β − actin and expressed in arbitrary units (A.U.). (D) Q-PCR analysis of the relative mRNA expression of the indicated cell cycle-related proteins, normalised to β-actin from 2 week old Wt and Tg mice (n = 3 in each case). (E) Representative immunoblots and quantitative histograms of protein expression levels normalised to β-actin of the indicated cell cycle-related proteins in 2 week old Wt and Tg mice (n = 3 in all cases). All data are presented as mean ± S.E. $^*P < 0.05$; ns: not significant.

(Fig. 5A) and an increase in nuclear cyclin D2 protein levels (Fig. 5B) when compared with AdβGal-transduced controls. Inhibition of ERK1/2 activation with PD98059 both decreased the basal level of expression of cyclin D2, and ablated the increases in cyclin D2 mRNA and protein levels upon Nox4 overexpression (Figs. 5C & D).

To test the functional significance of this Nox4-dependent increase in cyclin D2 expression upon cardiomyocyte proliferation, we silenced its expression in NRCs by siRNA. siRNA-mediated silencing resulted in an approximate 50% knockdown of cyclin D2 protein levels (Fig. 5E), and this depletion of cyclin D2 was sufficient to ablate the Nox4-induced increase in NRC proliferation (Fig. 5F). Therefore, the increase in cyclin D2 expression is a necessary mediator of the increase in NRC proliferation mediated by Nox4.

3.6. Nox4 activates cyclin D2 expression via ERK-dependent phosphorylation of c-myc

It is known that a key positive regulator of cyclin D2 transcription is c-myc [36,37] and that c-myc can be activated by phosphorylation of Thr58 and Ser 62 by ERK1/2 [38,39]. We determined the levels of both total and phospho-c-myc protein within the (2 week-old) Wt and Nox4 Tg hearts and found that ratio of phospho-c-myc: total c-myc was significantly increased in the Tg mouse hearts (Fig. 6A). Isolated NRCs transduced with AdNox4 *in vitro* similarly demonstrated a large increase in phospho-c-myc compared to AdβGal-transduced controls, and this increase was found to be ablated by ERK1/2 inhibition with PD98059 (Fig. 6B). Thus Nox4 overexpression increases c-myc phosphorylation and activation *via* ERK1/2 in cardiomyocytes.

To determine whether c-myc is acting to increase cyclin D2 expression in the NRCs, we silenced c-myc by siRNA (Figs. 6C & D) and this depletion of c-myc resulted in a significant decrease in cyclin D2 expression that was apparent upon Nox4 overexpression (Figs. 6E and F). Thus consistent with previous reports [36,37], we found c-myc to be a positive regulator of cyclin D2 transcription, and additionally to be (at least in part) responsible for mediating the Nox4-dependent increase in cyclin D2 expression.

3.7. Nox4-generated ROS increases the rate of cyclin D2 transcription via a highly conserved, cis-acting promoter region containing functional c-myc binding sites

To confirm the role of c-myc in the transcriptional regulation of cyclin D2, we investigated its functional effect on the proximal cyclin D2 promoter. We cloned a mouse genomic fragment, comprising this proximal promoter region (−15 bp to −1781 bp relative to the translational start site) upstream of a luciferase reporter gene (cyclin D2-luc). This

region shows a very high degree of homology between human and mouse, suggesting functional significance, and also includes a conserved binding site for c-myc which has been shown previously to function in the positive regulation of cyclin D2 transcription in murine fibroblasts [36,37] (Fig. 7A). Upon transfection into neonatal rat cardiomyocytes, this fragment was sufficient to direct a high level of transcriptional activation, confirming its promoter activity, and this activity was significantly increased, upon Nox4 overexpression. By contrast, Nox4 overexpression had no effect on the luciferase reporter activity resulting from a promoterless luciferase vector, pGL4.22 (Fig. 7B). Further, the increase in the cyclin D2 promoter activity upon Nox4 overexpression was significantly reduced in the presence of either c-myc siRNA or the inhibitor of ERK1/2 (Figs. 7C & D). Therefore within NRCs, Nox4-generated ROS stimulate ERK1/2 activation which results in increased

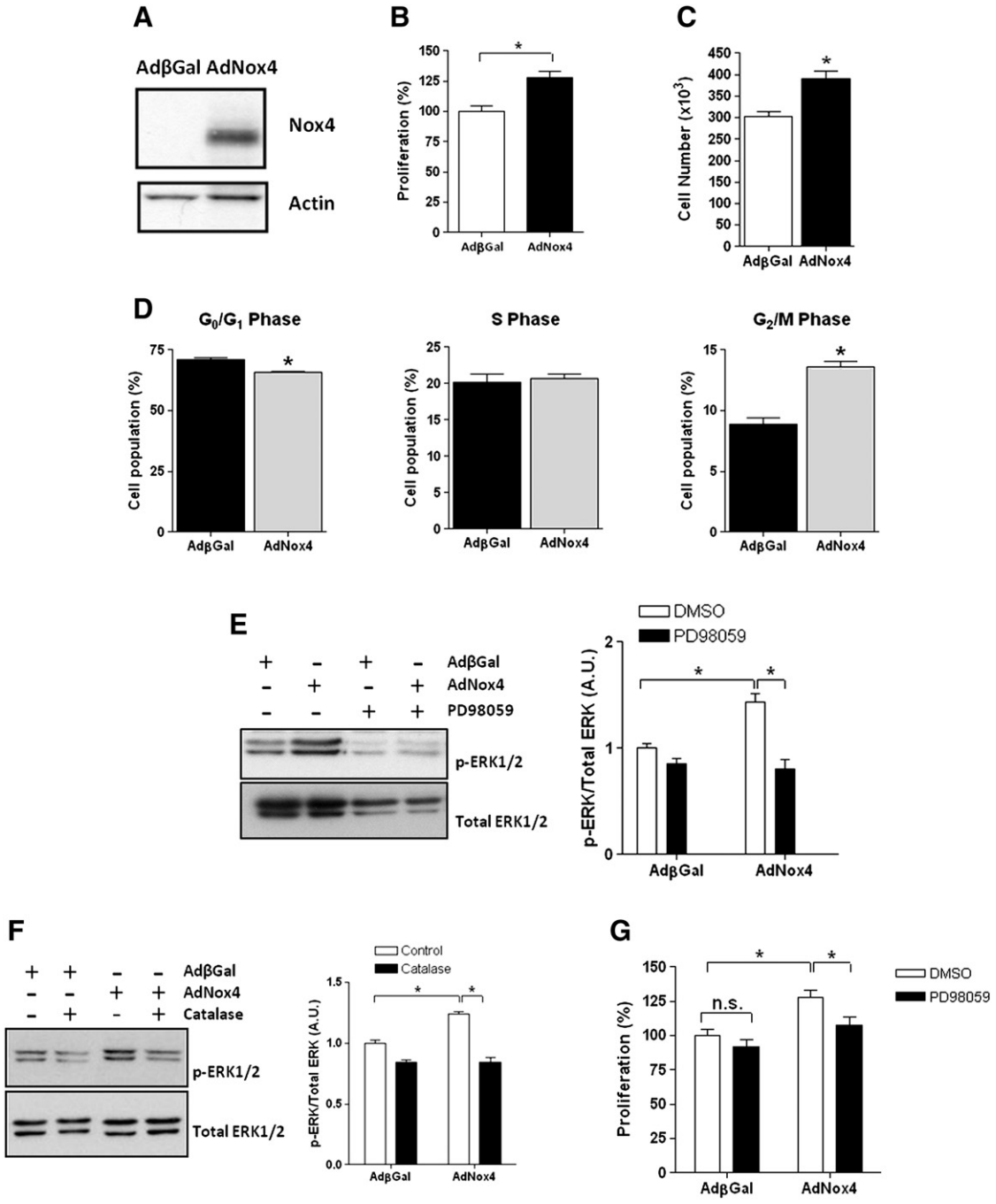

Fig. 4. Nox4 expression increased NRC proliferation *via* an ERK1/2-dependent pathway. NRCs were transduced with either Nox4 (AdNox4) or β-galactosidase (Ad βGal) and incubated for 30 h. (A) Immunoblot of Nox4 expression in transduced NRC cells. (B) MTS-based assessment of NRC proliferation after transduction with either AdNox4 or AdβGal (n = 3). (C) Physical cell count assessment of NRC proliferation after transduction with either AdNox4 or AdβGal (n = 3). (D) Cell cycle analysis of the G_0/G_1, S and G_2/M populations of NRCs after AdβGal or AdNox4 transduction (n = 3). (E & F) Representative immunoblots of phosphorylated and total ERK1/2 levels in NRCs after transduction with AdβGal or AdNox4 in the presence or absence of 20 μM PD98059 (E) or after catalase treatment (400 U/ml overnight; F). Histograms represent the ratio of phosphorylated ERK1/2 to total ERK1/2 protein levels in each case (n = 3). (G) MTS-based cell proliferation assay of NRCs after AdβGal or AdNox4 transduction in the presence or absence of 20 μM PD98059 (n = 3). (H) Cell cycle analysis of NRCs after AdβGal or AdNox4 transduction in the absence (vehicle) or presence of 20 μM PD98059 (n = 3). (I) Representative immunoblot and quantitative histogram showing increased ERK1/2 phosphorylation in 2 week-old Nox4 Tg hearts compared to Wt controls (n = 3). The histogram represents the ratio of phosphorylated ERK1/2 to total ERK1/2 protein levels. All data are presented as mean ± S.E. $^*P < 0.05$.

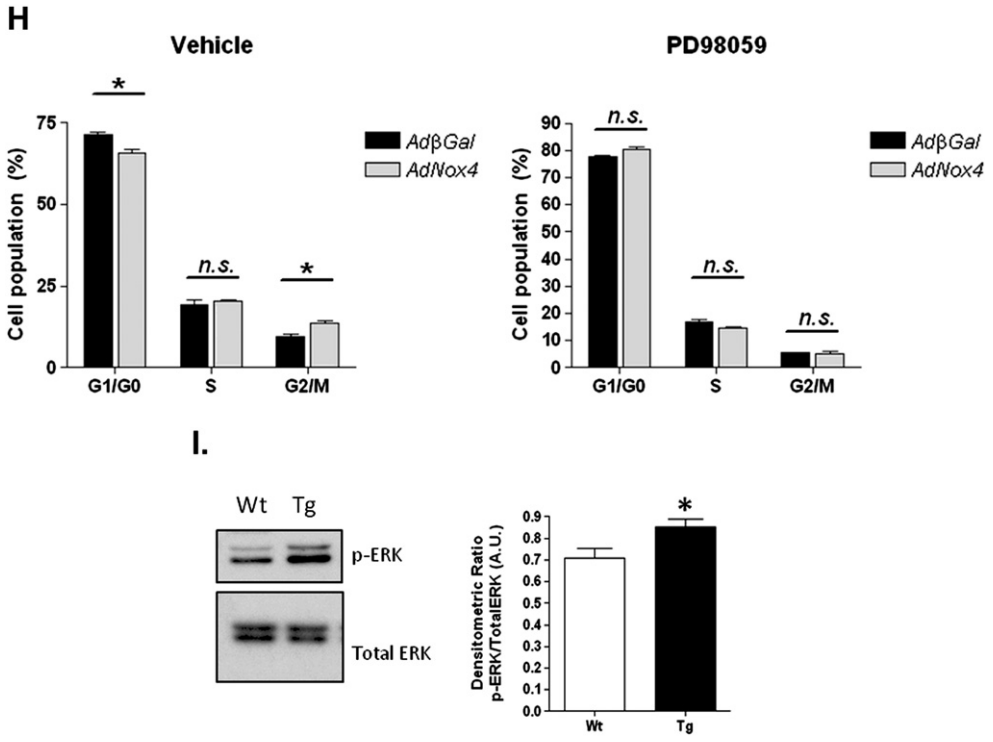

Fig. 4 (*continued*).

c-myc phosphorylation. c-Myc in turn acts to transactivate the cyclin D2 promoter *via* a *cis*-acting promoter element(s) to increase the rate of cyclin D2 transcription.

3.8. Overexpression of Nox4 in the postnatal heart prolongs the period of cardiomyocyte cell cycling

As mentioned above, the increased heart weight/body weight ratios of the Nox4 Tg hearts is transient. Thus we continue to observe significant differences in heart size at three and five week time points, but this phenotype is lost by seven weeks of age (Fig. 8A). We assessed the cell cycling status of the cardiomyocytes in the hearts of these mice, after 7 weeks of age. Immunological staining for the mitotic marker Ki67, together with the cardiomyocyte-specific troponin I sarcomeric protein, demonstrated that the Tg cardiomyocytes were no longer cycling at 7 weeks post-parturition (Fig. 8B). Thus at this time point Ki67 immunoreactivity was only apparent in non-cardiomyocyte cells. Further, BrdU incorporation into the cardiomyocyte nuclei was no longer apparent in cells isolated from either the Wt or Nox4 Tg mouse hearts (see Supplementary data, Fig. S3).

The transgenic expression of Nox4 (driven by the αMHC promoter) however remains at least as high in the adult (7 week) Tg mice as in the 2-week-old mice (Fig. 1A & [29]). Further, the (ROS-dependent) activation of ERK1/2 is sustained in the hearts of these adult Tg mice, compared to Wt littermate controls (Fig. 8C). In addition, cyclin D2 mRNA also remains overexpressed in the Tg adult mouse hearts, and this increase in transcription is reflected in a significant increase in cyclin D2 protein at this stage (Figs. 8D & E). By contrast however the protein levels of cdc2 and cdc6, which were elevated in the 2 week old hearts, are no longer increased in the adult Tg mouse hearts (see Supplementary data, Fig. S4). It has been shown that the nuclear trafficking of the D cyclins, including cyclin D2, is an important regulator of the cell cycle (reviewed in [40]). We therefore assessed the sub-cellular localisation of cyclin D2 in the Wt and Tg hearts at 2 days, 11 days and 7 weeks after birth. These data clearly show significant nuclear localisation of cyclin D2 in Wt and Tg mouse hearts that is lost in the Wt mice by 11 days, concomitant with the normal loss in cardiomyocyte cell cycling activity. By contrast, in the Tg mouse hearts, there remain significant levels of cyclin D2 at 11 days after birth (Figs. 8G, H). However no nuclear cyclin D2 is apparent in either Wt or Tg mouse hearts by 7 weeks of age (Fig. 8I). Therefore a loss in nuclear cyclin D2 localisation correlates with a loss in proliferative capacity in both Wt and Tg mouse hearts.

The loss of proliferative capacity of the cardiomyocytes in the adult Tg hearts however does not fully account for the normalisation of the heart sizes to those of the Wt animals. We therefore measured the dimensions of the cardiomyocytes isolated from these adult (male) mice. Adult cardiomyocytes from both the Wt and Tg cohorts were heterogeneous in size, and although there was a trend towards a smaller cell size in the Tg group, this was not significant (Fig. 8F). Similarly, the cell volumes of isolated adult cardiomyocytes assessed in a Coulter Counter were not found to be significantly different between the two groups (Supplementary data, Fig. S5). Although the accumulation of cardiomyocytes in the G_2/M cell cycle phase, upon ectopic expression of Nox4 is likely a result of increased progression through the G_1/S cell cycle phase (see Section 4, Discussion), it can also be an indicator of cellular senescence and/or apoptosis (reviewed in [41]). We therefore assessed the degree of senescence and apoptosis within young (8 day-old) and older (7 week-old) mice. No evidence of senescent cells was apparent in Wt or Tg mouse hearts at either time point (Supplementary data, Fig. S7), and only minimal levels of apoptosis were apparent in all cases (Supplementary data, Fig. S8). Thus, it appears that overexpression of Nox4 in the Tg cardiomyocytes prolongs the period of cardiomyocyte cell cycling and proliferation in the first 1–2 weeks after birth. This is not sustained into adulthood, and the loss of proliferative capacity correlates with a loss of nuclear-localisation of cyclin D2. The mechanistic cause of the normalisation of the heart sizes in the older Wt and Tg mice, however, remains to be elucidated.

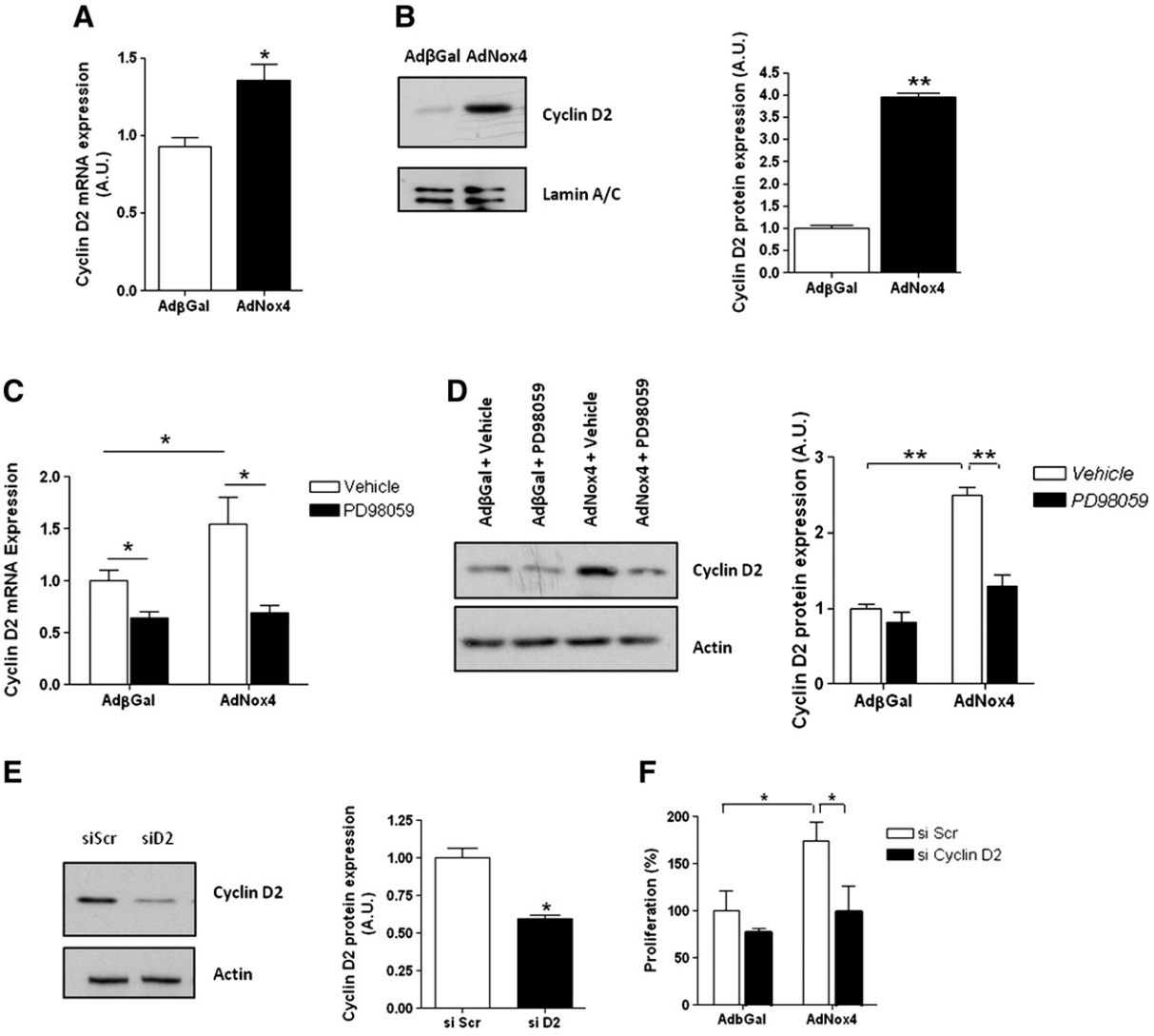

Fig. 5. Nox4-induced proliferation in NRCs is mediated by the transcriptional upregulation of cyclin D2. (A) Q-PCR analyses showing relative cyclin D2 mRNA expression, normalised to β-actin (n = 3) and (B) representative immunoblots and quantitative histograms of protein expression levels normalised to those of laminin A/C in NRCs transduced with either Nox4 (AdNox4) or β-galactosidase (AdβGal) as control, for 30 h (n = 3). (C) Q-PCR analyses of cyclin D2 mRNA levels in NRCs transduced with either AdNox4 or AdβGal for 30 h in the presence or absence of the MEK inhibitor, PD98059 (n = 3). (D) Representative immunoblot and quantitative histograms of cyclin D2 levels (relative to those of β-actin) in protein extracted from cells as described in (C) (n = 3). (E) Representative immunoblot and quantitative histogram of cyclin D2 protein in NRCs after either scrambled (siScr) or cyclin D2 (siD2) siRNA treatment (n = 3). (F) MTS-based cell proliferation assay of NRCs transduced with either AdNox4 or AdβGal for 30 h in the presence of scrambled, or cyclin D2 siRNA (n = 3). All data are presented as mean ± S.E. $^{*}P < 0.05$.

4. Discussion

4.1. The cardiomyocyte cell cycle is under redox control in vivo

Understanding the molecular mechanisms which underlie the regulation of the cardiomyocyte cell cycle is crucial in further developing strategies to regenerate and repair cardiac tissue after ischemic or hemodynamic insult. Mammalian cardiomyocytes exit from the cell cycle shortly after birth. The data presented here demonstrate that the cardiomyocyte cell cycle is, in part, under redox regulation *in vivo*. Previous studies had demonstrated that exogenous administration of H_2O_2 to mouse neonatal cardiomyocytes promoted proliferation *in vitro* [10], and we show here that cardiac-specific overexpression of an enzymatic, endogenous source of H_2O_2 (Nox4), can act crucially *in vivo*, to promote cardiomyocyte cell cycling in the postnatal heart. Thus the Nox4 Tg mouse pup hearts were larger than Wt litter mate controls, while the volumes of the individual cardiomyocytes were slightly, but significantly, smaller, and displayed higher rates of DNA synthesis. A striking feature of the transcriptome of the Nox4 Tg mouse heart is a very significant increase in cyclin D2 mRNA. We propose that this increase in cyclin D2 expression is critical to the increased cardiomyocyte cycling seen in these Tg pups, and underlies their overt cardiac hyperplasia. Thus cardiac-specific ectopic expression of cyclin D2 *per se* in transgenic mice has previously been demonstrated to be sufficient to increase heart size and prolong cardiomyocyte cell cycling activity, as judged by sustained DNA synthesis in cardiomyocytes in the adult heart [33]. Crucially, ectopic cardiac-specific expression of cyclin D2 has also been shown to result in enhanced cardiac growth in the postnatal period due to increased cardiomyocyte proliferation [24], as we suggest in our Nox4 Tg model. Further, overexpression of cyclin D2 in NRCs *in vitro* has similarly been shown to be sufficient to increase DNA synthesis and cell cycling [31], and we demonstrate here that inhibition of cyclin D2 expression by siRNA was sufficient in NRCs to ablate the increase in cell proliferation apparent upon Nox4 transduction.

Previous reports however have argued about the relative importance of either cyclin D1 or cyclin D2 in driving the progression of the cardiomyocyte cell cycle [42]. As has been shown for cyclin D2, cyclin D1 is also known to increase cardiomyocyte cell cycling activity

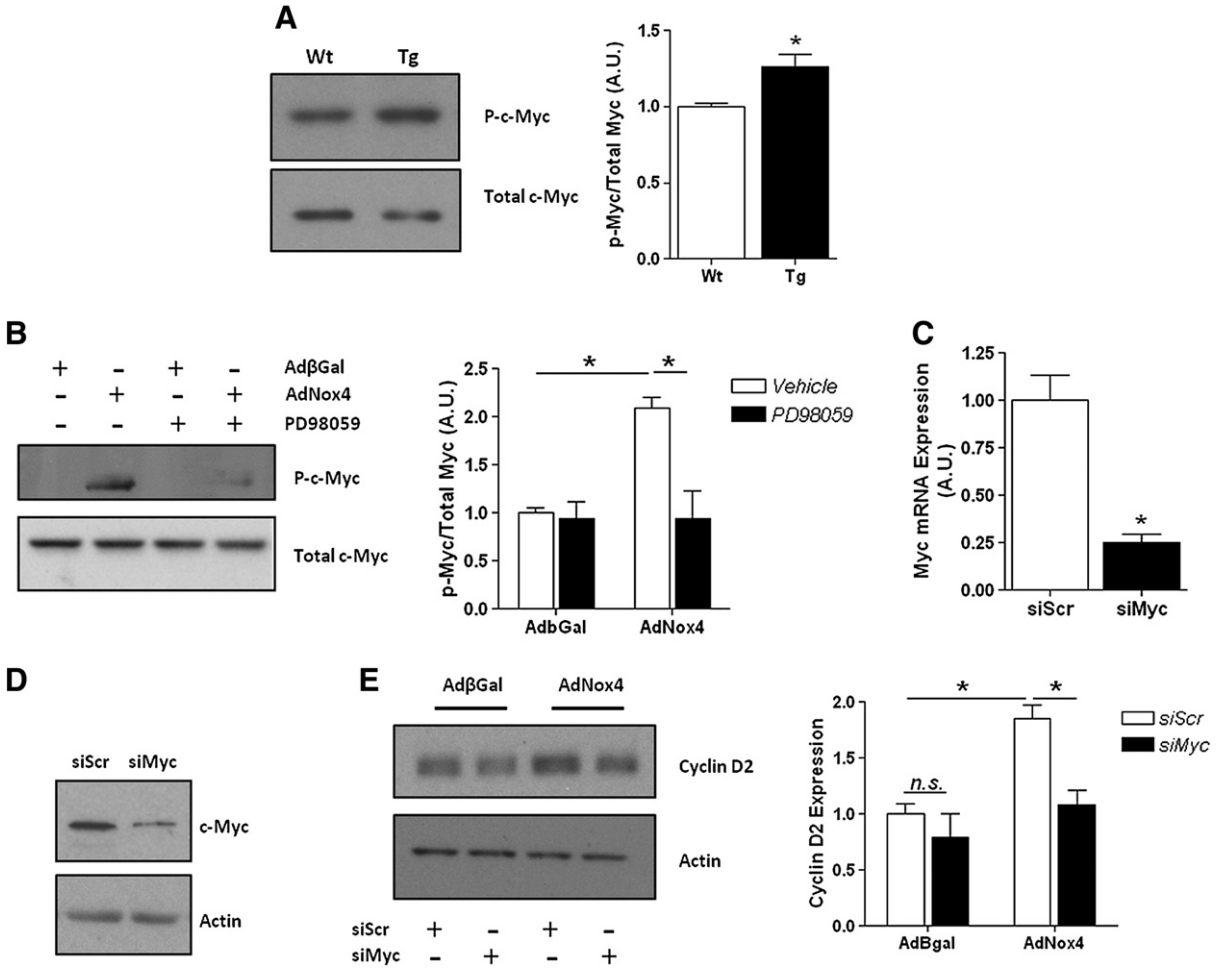

Fig. 6. Nox4 overexpression activates c-myc resulting in increased cyclin D2 expression. (A) Representative immunoblot showing increased c-myc phosphorylation in 2 week-old Nox4 Tg hearts compared with Wt littermate controls. The histogram represents the ratio of phosphorylated c-myc to total c-myc protein levels (n = 3). (B) Representative immunoblot and quantitative histogram showing phosphorylated and total c-myc levels in NRCs transduced with either AdNox4 or AdβGal for 30 h in the presence or absence of PD98059 as indicated (n = 3). (C) Q-PCR analyses of c-myc mRNA expression, relative to that of β-actin (n = 3), and (D) representative immunoblot indicating c-myc protein expression, in NRCs after 48 h of c-myc siRNA treatment as indicated. β-Actin is shown as a loading control for protein expression. (E) Representative immunoblot and quantitative histogram showing cyclin D2 protein expression, relative to that of β-actin, in NRCs transduced with either AdNox4 or AdβGal for 30 h in the presence of scrambled or c-myc siRNA as indicated (n = 3). All data are presented as mean ± S.E. $^{*}P < 0.05$.

in vitro [43], and transgenic mice models of cardiac-specific cyclin D1 or D2 overexpression clearly demonstrate that both induce increased cardiomyocyte cycling activity *in vivo* [23,33]. Cyclin D1 has also previously been suggested to be regulated by H_2O_2, *via* redox-dependent stabilisation of the cyclin D1 protein [44]. However, we found no evidence of increased cyclin D1 expression, at the level of either mRNA or protein, in the hearts of the 2 week old Nox4 Tg mice, suggesting that cyclin D1 is not the mediator of the increased cardiomyocyte proliferation in this mouse model (Supplementary data, Fig. S6).

We therefore aimed to elucidate *in vitro* the redox-dependent mechanisms underlying the positive regulation of cyclin D2 transcription and cell proliferation seen upon Nox4 overexpression in NRCs. We show here a (Nox4-generated) ROS-dependent activation of the ERK1/2 signalling pathway that mediates increased phosphorylation and activation of c-myc, upregulation of cyclin D2 (mRNA and protein) expression and enhanced cardiomyocyte proliferation *in vitro*. This is consistent with previous reports which have demonstrated activation of the ERK1/2 signalling pathway by Nox4 in other cell types both *in vitro* [34,45] and *in vivo* [46], while ERK1/2 activation is associated with increased cellular proliferation in various other cellular settings (reviewed in [47]). Further, we present evidence that the Nox4-dependent increase in cyclin D2 expression was dependent upon the direct activation of its transcription *via* the binding of c-myc to known conserved binding site(s) within its proximal promoter region [37,48]. However, this does not exclude the potential involvement of other redox-regulated transcription factors in the activation of cyclin D2 expression by Nox4. Thus Sp1 and Stat5 are also known positive regulators of the cyclin D2 promoter (Fig. 7A) [48], that are potentially regulated by ROS *via* ERK1/2 activation [49,50] and may additionally contribute to the full upregulation observed.

There have been several, sometimes conflicting, reports of the role of Nox4 in cellular proliferation in diverse cell types. Thus ablation of Nox 4 in melanoma cells has been shown to inhibit proliferation, *via* regulation of G_2-M cell cycle progression [51], while in airway smooth muscle cells Nox4 was shown to be a positive mediator of TGF-β1-induced proliferation. In the latter case the Nox4 was shown to influence cell cycle transition through both G_1/S and G_2/M [52]. By contrast, in hepatocytes ablation of Nox4 resulted in increased cell proliferation and resulted in a higher proportion of cells in S and G_2/M phases [53]. The differences in these observations likely reflect both differences in subcellular localisation of Nox4 and/or intracellular composition of targets of ROS and associated signalling components between the different cell types. We demonstrate here, that in cardiomyocytes Nox4-generated ROS is a positive mediator of cell cycling, and that the increased proliferation is associated with a lower proportion of cells in G_0/G_1, and a concomitant increase in cell in the G_2/M cell cycle phase. These results are

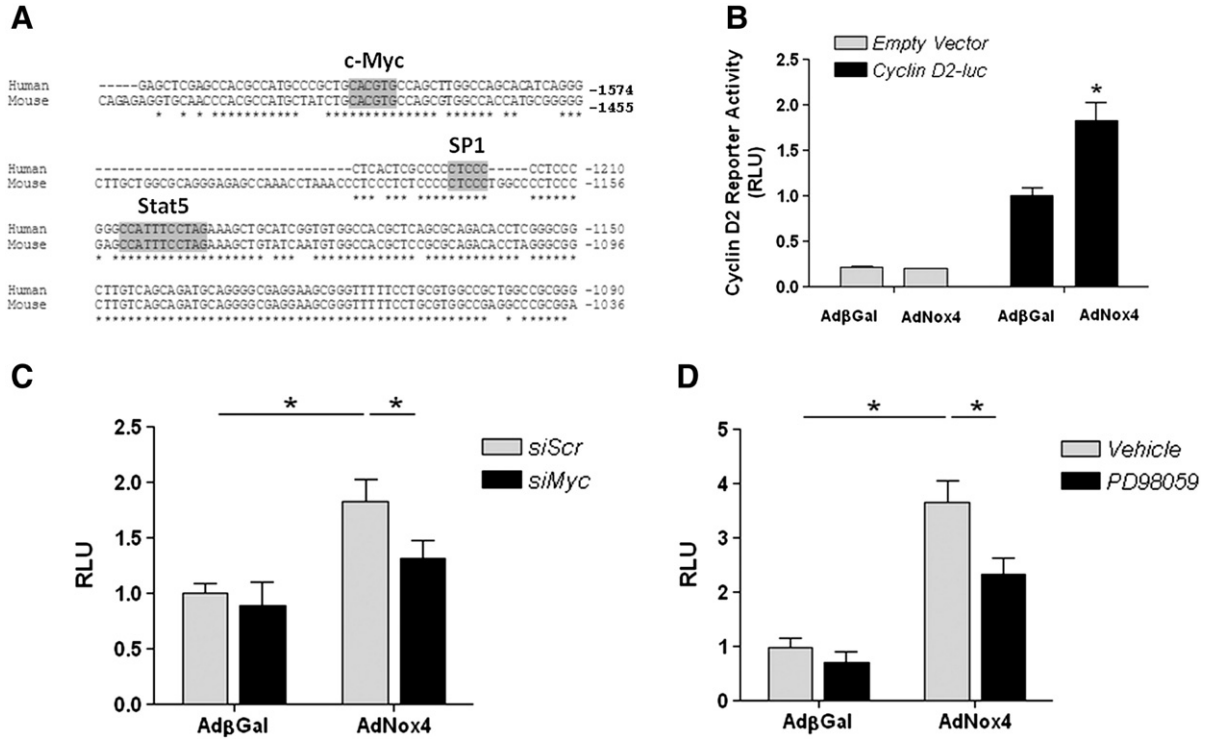

Fig. 7. Nox4-generated ROS increases the rate of cyclin D2 transcription *via* a highly conserved, *cis*-acting promoter fragment. (A) A DNA sequence comparison showing high conservation between regions of the proximal human and mouse cyclin D2 promoter regions, upstream of exon 1. Functional binding sites for indicated transcription factors [37,48] are indicated and shaded in grey. Stars indicate nucleotide homology between species. Nucleotides are numbered relative to start of translation of each gene. (B) Relative luciferase activity (RLA) resulting from a promoterless firefly luciferase vector (empty vector) or from a construct comprising a 1766 bp genomic fragment of the proximal mouse cyclin D2 promoter ligated upstream of the luciferase reporter gene (cyclin D2-luc) in NRCs transduced with either AdNox4 or AdβGal for 28 h. (C & D) RLA resulting from the cyclin D2-luc in NRCs transduced with either AdNox4 or AdβGal for 28 h in the presence of scrambled or cmyc siRNA(C), or PD90859 (D), as indicated. In each case, luciferase activities are normalised to that of a co-transfected *Renilla* luciferase vector and expressed as relative luminescence units (RLUs; n = 3). The RLU resulting from cyclin D2-luc transduced with AdβGal was set to 1.0 in each case. All data are presented as mean ± S.E. $^{*}P < 0.05$.

consistent with the notion that the associated increase in cyclin D2 expression, seen upon Nox4 overexpression, is acting to promote the G_1/S phase transition in the cardiomyocytes, as has been reported previously in other cell types [54].

The *in vitro* observations of increased ERK1/2 phosphorylation and increased c-myc phosphorylation accompanying the increased cyclin D2 expression were also mirrored *in vivo* in the Nox4 Tg mouse hearts, suggesting an equivalent ERK1/2-dependent molecular pathway. Therefore our data may be consistent with, and build upon, a previous report in which cardiac-specific overexpression of insulin-like growth factor 1B (IGF-1B) resulted in increased postnatal cardiomyocyte proliferation [55]. IGF-1B has been shown to both induce ROS production mediated by Nox4 [56], and to activate ERK1/2 [57]. Thus it seems likely that Nox4 may be involved in the increased cardiomyocyte cell cycling observed in this mouse model. It may also be highly significant that inappropriate ERK1/2 hyperphosphorylation in embryonic hearts has been shown previously to result in congenital cardiac defects resulting from altered cardiomyocyte cell cycling [58]. The cardiac-specific expression of Nox4 in our Tg mouse model is driven by the αMHC promoter, which is not activated in the embryo, but directs expression only in the postnatal animal [29]. It may be that embryonic-stage cardiomyocytes, which are already very proliferative, have an increased susceptibility to and are therefore less tolerant of, increased ERK1/2 activation.

In this mouse model, Nox4 overexpression appears to prolong the period of cardiomyocyte proliferation soon after birth, but was not sufficient, in the adult mouse to maintain increased cardiomyocyte cell-cycling. In this respect, the phenotype of the Nox4 Tg mouse is similar to that of the p27KIP1 knockout mouse. Thus ablation of the cell cycle inhibitor, p27KIP1, allowed additional rounds of proliferation in the cardiac myocyte population of neonatal mice but was not, in itself, sufficient to prevent exit from the cell cycle [59]. Clearly, a multitude of factors are needed to overcome cardiac cell cycle arrest and promote full cellular proliferation in the adult heart. The enlarged heart size in the Nox4 Tg mice was progressively lost before 7 weeks of age, despite a sustained increase in ERK1/2 activation and cyclin D2 (mRNA and protein) expression. One might predict that this "normalisation" in the heart size might reflect less hypertrophic growth in the (more numerous) Nox4 Tg cardiomyocytes, and therefore the average cardiomyocyte size would be significantly smaller in the Nox4 Tg adult mice, compared to age-matched Wt controls. Perhaps surprisingly, however, we found no significant differences in the mean cardiomyocyte volumes, either by taking physical measurements of isolated cells or by taking measurements on a Coulter Counter. The complex mechanisms whereby cells and organs maintain size homeostasis are poorly understood, and must involve the coordinated regulation of cell growth, proliferation and survival pathways [60], and would need to be extensively examined to fully explain our observations here.

Not surprisingly, these Nox4 Tg mice show striking phenotypic similarities to cardiac-specific cyclin D2 Tg mice [24,32]. In particular in one study, cyclin D2 overexpression was specifically shown to increase proliferation in the postnatal heart, resulting in increased cardiac growth, as we describe here [24]. However in both these studies the increased heart weight: body weight ratio, and increased cardiomyocyte DNA synthesis persisted into the adult. By contrast both these phenotypes were lost in the Nox4 Tg mice by 7 weeks of age, and we demonstrate this to correlate with the complete loss of cyclin D2 localised within the nucleus. It is notable that in the cyclin D2 Tg mice described, a very high level of expression of the transgene (driven by the αMHC promoter) was achieved, and some nuclear expression of cyclin D2 was observed in the adult mouse [32]. Therefore the differences in levels of

cyclin D2 expression between the two Tg mouse models are likely to account for these differences. Interestingly, the cardiac-specific cyclin D2 transgenic mouse has been shown to be cardiac-protective in a number of different assays. Thus it demonstrated increased cardiomyocyte cycling after permanent coronary arterial occlusion, with a subsequence regression in infarct size and an improvement in cardiac function [61]

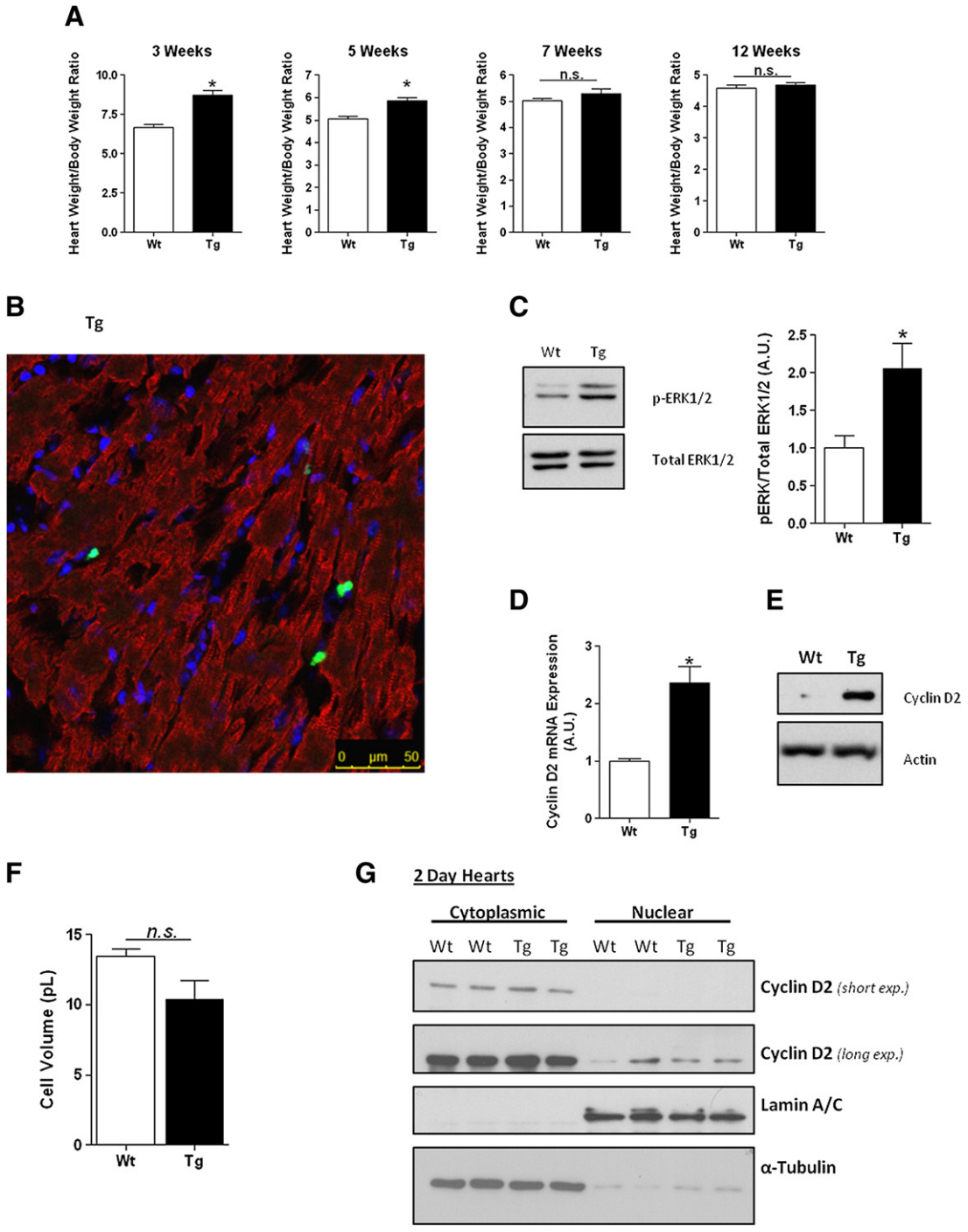

Fig. 8. Forced expression of Nox4 in the postnatal heart prolongs the period of myocyte proliferation. (A) Quantification of heart/body weight ratios of Wt and Nox4 Tg mice at 3 weeks (n = 3/4), 5 weeks (n = 6/6), 7 weeks (n = 13/9) and 12 weeks (n = 13/13) post-birth. *$P < 0.05$, 2-tailed Student's *t*-test. Ns: not significant. Heart/body weight ratios of 5 week and 7 week-old Wt and Tg mice additionally analysed by one-way ANOVA with Bonferroni post-hoc test showed significant change at 5 weeks ($P < 0.05$) are lost at 7 weeks. (B) Representative immunofluorescence staining of transverse frozen heart sections from 7 week old Nox4 Tg mice co-stained with an antibody against the proliferation marker Ki67 (green), cardiac troponin T (red) and the cell nuclei stain DAPI (blue). No Ki67-positive cardiomyocytes are visible at this time point. Scale bar, 50 µm. (C) Representative blot and quantitative histogram showing increased ERK1/2 phosphorylation in 7 week old Nox4 Tg hearts when compared with Wt controls. The histogram represents the ratio of phosphorylated ERK1/2 to total ERK1/2 protein levels (n = 3). (D) Q-PCR analyses of cyclin D2 mRNA levels in 7 week old Wt and Nox4 Tg mice, relative to levels of β-actin mRNA (n = 3). (E) Representative immunoblot showing cyclin D2 protein expression levels in 7 week old Wt and Nox4 Tg mice, compared to those of β-actin. (F) Histogram indicating cell volumes in pico litres (pl) of Wt and Nox4 Tg adult cardiomyocytes isolated from 13 week old male mice (n = 3/3). Cell volumes were assessed by physical measurements of length and cross sectional diameter, and subsequent calculation of volume based on these parameters (see Section 2, Materials and methods). (C, D, F) *$P < 0.05$, 2-tailed Student's *t*-test. Ns: not significant. (G, H, I) Representative immunoblots demonstrating cytoplasmic and nuclear localisation of cyclin D2 in Wt and Nox4 Tg mouse hearts at 2 days (G), 11 days (H) and 7 weeks (I) after birth. Staining for lamin A/C and α-tubulin demonstrates successful fractionation of nuclear and cytoplasmic proteins, respectively. Nuclear cyclin D2 is apparent in Wt and Tg mouse hearts at 2 days, and in Tg hearts only at 11 days after birth. No nuclear cyclin D2 is apparent in Wt or Tg hearts of the adult mice.

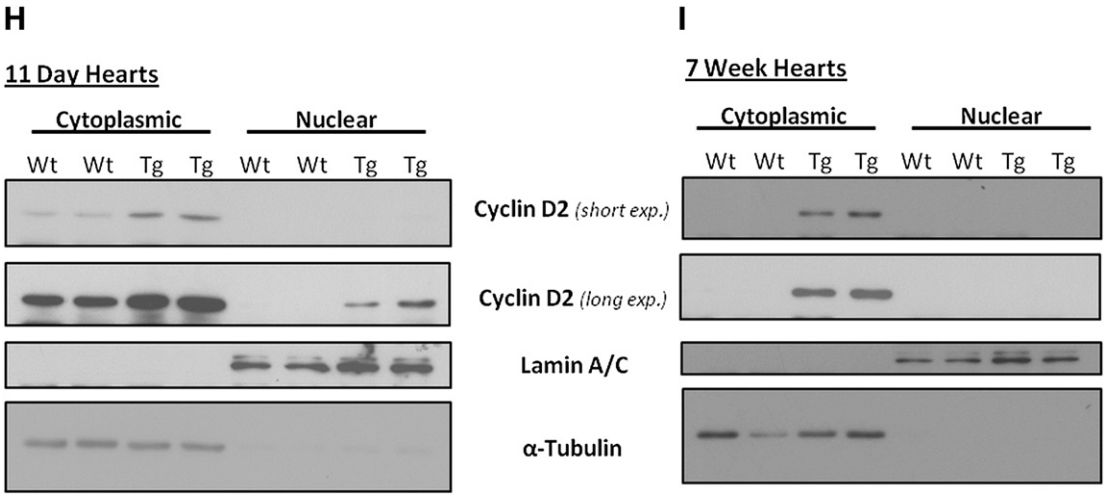

Fig. 8 (*continued*).

This increased cell cycling activity has also been shown to antagonise myocardial fibrosis resulting from cardiac-specific TGFβ-overexpression [62]. The finding that in the present study Nox4-overexpression acts to increase cyclin D2 expression therefore warrants investigation of its effects on cardiac function and adaptation in disease models.

The elucidation of the molecular pathway modulating the ROS-dependent increase in cardiomyocyte cycling offers the possibility of targeting components of this pathway therapeutically. One promising potential target is the protein tyrosine phosphatase *Src* homology region 2, phosphatase 2 (SHP2). SHP2 is known to be a positive mediator of ERK1/2 signalling, and cardiac-specific increased activity of SHP2 leads to increased cardiomyocyte cell cycling and resultant defects within the embryonic heart. However, in the postnatal heart SHP2 hyperactivity is completely benign [58]. Although the cycling capacity of the cardiomyocytes was not assessed in these experiments, the ERK1/2 activation mediated by the increased SHP2 activity was shown to be upregulated in the postnatal mouse hearts. The transcriptional regulation of cyclin D2 by c-myc may also be a mechanism affording therapeutic intervention. The binding of c-myc to the cyclin D2 promoter is known to depend on the dimerization with a partner protein, Max, which is inhibited by histone deacetylase (HDAC) activity, and enhanced by histone acetyl transferase (HAT) complexes [36,37]. Thus appropriate small molecule modulators of HDAC/HAT activities [63,64] may prove therapeutically useful in helping to promote cardiomyocyte cycling after ischaemic injury.

The question as to the endogenous source(s) of ROS which may modulate cardiomyocyte cell cycling *in vivo* is not fully addressed here. The family of NADPH oxidases, and in particular Nox4 seems a likely candidate to effect this redox regulation in cardiomyocytes *in vivo*. However, Nox4 KO mice show no obvious defect in cardiac structure or function under "baseline" physiological conditions [16], suggesting that Nox4 may not have an obligatory role. Nevertheless, the observation that endogenous Nox4 expression declines sharply after birth, together with the potential for the Nox4-mediated, enhancement of cardiomyocyte proliferation demonstrated here, suggest that redox signalling mediated by Nox4 may be an important pro-proliferative mechanism that becomes downregulated and contributes to cardiomyocyte cycle arrest in the postnatal mammalian heart.

4.2. Conclusions

The cardiomyocyte cell cycle is regulated by redox-dependent signalling pathway(s) *in vivo*. Nox4 is demonstrated here to be an important potential source of ROS mediating such pathways, and overexpression of Nox4 results in increased cardiomyocyte cell cycling in the heart soon after birth. *In vitro* we demonstrate a pathway leading to increased cardiomyocyte proliferation, in which Nox4-generated ROS acts to mediate ERK1/2 activation and subsequent phosphorylation of the transcription factor c-myc. c-Myc in turn acts to upregulate cyclin D2 expression, which is known to be both necessary and sufficient to drive cardiomyocyte proliferation *in vitro*. We present evidence that this same pathway acts *in vivo* to increase cardiomyocyte cell cycling upon Nox4 overexpression.

Supplementary data to this article can be found online at http://dx.doi.org/10.1016/j.yjmcc.2014.10.017.

Sources of funding

This work was supported by grants from the British Heart Foundation (BHF), nos. PG/08/110/26228 and RG/08/110/25922, and a BHF Centre of Excellence Award — RE/13/2/30182. This study is also supported by a Foundation Leducq Transatlantic Network of Excellence Award grant no. 09CVD01 and the Department of Health *via* a National Institute for Health Research (NIHR) Biomedical Research Centre Award to Guy's and St. Thomas' NHS Foundation Trust in partnership with King's College London and King's College Hospital NHS Foundation Trust. M.S. is funded by the German Research Foundation DFG grant no. IRTG1816.

Disclosures

None.

Acknowledgments

We would like to acknowledge Thomas Leto for the kind gift of full-length mouse Nox4 cDNA and Shiney Reji for the technical assistance.

References

[1] Bicknell KA, Coxon CH, Brooks G. Can the cardiomyocyte cell cycle be reprogrammed? J Mol Cell Cardiol 2007;42:706–21.
[2] Drenckhahn JD, Schwarz QP, Gray S, Laskowski A, Kiriazis H, Ming Z, et al. Compensatory growth of healthy cardiac cells in the presence of diseased cells restores tissue homeostasis during heart development. Dev Cell 2008;15:521–33.
[3] Porrello ER, Mahmoud AI, Simpson E, Hill JA, Richardson JA, Olson EN, et al. Transient regenerative potential of the neonatal mouse heart. Science 2011;331:1078–80.
[4] Ahuja P, Sdek P, MacLellan WR. Cardiac myocyte cell cycle control in development, disease, and regeneration. Physiol Rev 2007;87:521–44.
[5] Chiu J, Dawes IW. Redox control of cell proliferation. Trends Cell Biol 2012;22:592–601.
[6] Jones NC, Fedorov YV, Rosenthal RS, Olwin BB. ERK1/2 is required for myoblast proliferation but is dispensable for muscle gene expression and cell fusion. J Cell Physiol 2001;186:104–15.

[7] Meloche S, Pouyssegur J. The ERK1/2 mitogen-activated protein kinase pathway as a master regulator of the G1- to S-phase transition. Oncogene 2007;26:3227–39.
[8] Yamakawa T, Tanaka S, Kamei J, Kadonosono K, Okuda K. Pitavastatin inhibits vascular smooth muscle cell proliferation by inactivating extracellular signal-regulated kinases 1/2. J Atheroscler Thromb 2003;10:37–42.
[9] Chiarugi P. PTPs versus PTKs: the redox side of the coin. Free Radic Res 2005;39: 353–64.
[10] Buggisch M, Ateghang B, Ruhe C, Strobel C, Lange S, Wartenberg M, et al. Stimulation of ES-cell-derived cardiomyogenesis and neonatal cardiac cell proliferation by reactive oxygen species and NADPH oxidase. J Cell Sci 2007;120:885–94.
[11] Sauer H, Neukirchen W, Rahimi G, Grunheck F, Hescheler J, Wartenberg M. Involvement of reactive oxygen species in cardiotrophin-1-induced proliferation of cardiomyocytes differentiated from murine embryonic stem cells. Exp Cell Res 2004;294:313–24.
[12] Przybyt E, Krenning G, Brinker MG, Harmsen MC. Adipose stromal cells primed with hypoxia and inflammation enhance cardiomyocyte proliferation rate in vitro through STAT3 and Erk1/2. J Transl Med 2013;11:39.
[13] Santos CX, Anilkumar N, Zhang M, Brewer AC, Shah AM. Redox signaling in cardiac myocytes. Free Radic Biol Med 2011;50:777–93.
[14] Bedard K, Krause KH. The NOX family of ROS-generating NADPH oxidases: physiology and pathophysiology. Physiol Rev 2007;87:245–313.
[15] Chan EC, Jiang F, Peshavariya HM, Dusting GJ. Regulation of cell proliferation by NADPH oxidase-mediated signaling: potential roles in tissue repair, regenerative medicine and tissue engineering. Pharmacol Ther 2009;122:97–108.
[16] Zhang M, Brewer AC, Schroder K, Santos CX, Grieve DJ, Wang M, et al. NADPH oxidase-4 mediates protection against chronic load-induced stress in mouse hearts by enhancing angiogenesis. Proc Natl Acad Sci U S A 2010;107:18121–6.
[17] Ago T, Kuroda J, Pain J, Fu C, Li H, Sadoshima J. Upregulation of Nox4 by hypertrophic stimuli promotes apoptosis and mitochondrial dysfunction in cardiac myocytes. Circ Res 2010;106:1253–64.
[18] Heymes C, Bendall JK, Ratajczak P, Cave AC, Samuel JL, Hasenfuss G, et al. Increased myocardial NADPH oxidase activity in human heart failure. J Am Coll Cardiol 2003; 41:2164–71.
[19] Takac I, Schroder K, Zhang L, Lardy B, Anilkumar N, Lambeth JD, et al. The E-loop is involved in hydrogen peroxide formation by the NADPH oxidase Nox4. J Biol Chem 2011;286:13304–13.
[20] Serrander L, Cartier L, Bedard K, Banfi B, Lardy B, Plastre O, et al. NOX4 activity is determined by mRNA levels and reveals a unique pattern of ROS generation. Biochem J 2007;406:105–14.
[21] Pasumarthi KB, Field LJ. Cardiomyocyte cell cycle regulation. Circ Res 2002;90: 1044–54.
[22] Kozar K, Ciemerych MA, Rebel VI, Shigematsu H, Zagozdzon A, Sicinska E, et al. Mouse development and cell proliferation in the absence of D-cyclins. Cell 2004;118:477–91.
[23] Soonpaa MH, Koh GY, Pajak L, Jing S, Wang H, Franklin MT, et al. Cyclin D1 overexpression promotes cardiomyocyte DNA synthesis and multinucleation in transgenic mice. J Clin Invest 1997;99:2644–54.
[24] Yamak A, Temsah R, Maharsy W, Caron S, Paradis P, Aries A, et al. Cyclin D2 rescues size and function of GATA4 haplo-insufficient hearts. Am J Physiol Heart Circ Physiol 2012;303:H1057–66.
[25] Andrews NC, Faller DV. A rapid micropreparation technique for extraction of DNA-binding proteins from limiting numbers of mammalian cells. Nucleic Acids Res 1991;19:2499.
[26] Larkin MA, Blackshields G, Brown NP, Chenna R, McGettigan PA, McWilliam H, et al. Clustal W and Clustal X version 2.0. Bioinformatics 2007;23:2947–8.
[27] Murray TV, Smyrnias I, Shah AM, Brewer AC. NADPH oxidase 4 regulates cardiomyocyte differentiation via redox activation of c-Jun and the cis-regulation of GATA-4 transcription. J Biol Chem 2013;288(22):15745–59.
[28] Antoons G, Mubagwa K, Nevelsteen I, Sipido KR. Mechanisms underlying the frequency dependence of contraction and [Ca(2+)](i) transients in mouse ventricular myocytes. J Physiol 2002;543:889–98.
[29] Brewer AC, Murray TV, Arno M, Zhang M, Anilkumar NP, Mann GE, et al. Nox4 regulates Nrf2 and glutathione redox in cardiomyocytes in vivo. Free Radic Biol Med 2011;51:205–15.
[30] Zhong W, Mao S, Tobis S, Angelis E, Jordan MC, Roos KP, et al. Hypertrophic growth in cardiac myocytes is mediated by myc through a cyclin D2-dependent pathway. EMBO J 2006;25:3869–79.
[31] Busk PK, Hinrichsen R, Bartkova J, Hansen AH, Christoffersen TE, Bartek J, et al. Cyclin D2 induces proliferation of cardiac myocytes and represses hypertrophy. Exp Cell Res 2005;304:149–61.
[32] Pasumarthi KB, Nakajima H, Nakajima HO, Soonpaa MH, Field LJ. Targeted expression of cyclin D2 results in cardiomyocyte DNA synthesis and infarct regression in transgenic mice. Circ Res 2005;96:110–8.
[33] Borlado LR, Mendez J. CDC6: from DNA replication to cell cycle checkpoints and oncogenesis. Carcinogenesis 2008;29:237–43.
[34] Anilkumar N, Weber R, Zhang M, Brewer A, Shah AM. Nox4 and nox2 NADPH oxidases mediate distinct cellular redox signaling responses to agonist stimulation. Arterioscler Thromb Vasc Biol 2008;28:1347–54.
[35] Mebratu Y, Tesfaigzi Y. How ERK1/2 activation controls cell proliferation and cell death: is subcellular localization the answer? Cell Cycle 2009;8:1168–75.
[36] Bouchard C, Thieke K, Maier A, Saffrich R, Hanley-Hyde J, Ansorge W, et al. Direct induction of cyclin D2 by myc contributes to cell cycle progression and sequestration of p27. EMBO J 1999;18:5321–33.
[37] Bouchard C, Dittrich O, Kiermaier A, Dohmann K, Menkel A, Eilers M, et al. Regulation of cyclin D2 gene expression by the myc/max/mad network: myc-dependent TRRAP recruitment and histone acetylation at the cyclin D2 promoter. Genes Dev 2001;15:2042–7.
[38] Alvarez E, Northwood IC, Gonzalez FA, Latour DA, Seth A, Abate C, et al. Pro-Leu-Ser/Thr-Pro is a consensus primary sequence for substrate protein phosphorylation. Characterization of the phosphorylation of c-myc and c-jun proteins by an epidermal growth factor receptor threonine 669 protein kinase. J Biol Chem 1991;266: 15277–85.
[39] Sears R, Nuckolls F, Haura E, Taya Y, Tamai K, Nevins JR. Multiple Ras-dependent phosphorylation pathways regulate myc protein stability. Genes Dev 2000;14: 2501–14.
[40] Diehl JA. Cycling to cancer with cyclin D1. Cancer Biol Ther 2002;1:226–31.
[41] Houtgraaf JH, Versmissen J, van der Giessen WJ. A concise review of DNA damage checkpoints and repair in mammalian cells. Cardiovasc Revasc Med 2006;7:165–72.
[42] Tamamori-Adachi M, Goto I, Yamada K, Kitajima S. Differential regulation of cyclin D1 and D2 in protecting against cardiomyocyte proliferation. Cell Cycle 2008;7: 3768–74.
[43] Tamamori-Adachi M, Ito H, Nobori K, Hayashida K, Kawauchi J, Adachi S, et al. Expression of cyclin D1 and CDK4 causes hypertrophic growth of cardiomyocytes in culture: a possible implication for cardiac hypertrophy. Biochem Biophys Res Commun 2002;296:274–80.
[44] Martinez Munoz C, Post JA, Verkleij AJ, Verrips CT, Boonstra J. The effect of hydrogen peroxide on the cyclin D expression in fibroblasts. Cell Mol Life Sci 2001;58:990–6.
[45] Sturrock A, Cahill B, Norman K, Hueckstead TP, Hill K, Sanders K, et al. Transforming growth factor-beta1 induces Nox4 NAD(P)H oxidase and reactive oxygen species-dependent proliferation in human pulmonary artery smooth muscle cells. Am J Physiol Lung Cell Mol Physiol 2006;290:L661–73.
[46] Gorin Y, Block K, Hernandez J, Bhandari B, Wagner B, Barnes JL, et al. Nox4 NAD(P)H oxidase mediates hypertrophy and fibronectin expression in the diabetic kidney. J Biol Chem 2005;280:39616–26.
[47] Roskoski Jr R. ERK1/2 MAP kinases: structure, function, and regulation. Pharmacol Res 2012;66:105–43.
[48] Martino A, Holmes JHT, Lord JD, Moon JJ, Nelson BH. Stat5 and Sp1 regulate transcription of the cyclin D2 gene in response to IL-2. J Immunol 2001;166:1723–9.
[49] Merchant JL, Du M, Todisco A. Sp1 phosphorylation by Erk 2 stimulates DNA binding. Biochem Biophys Res Commun 1999;254:454–61.
[50] Pircher TJ, Petersen H, Gustafsson JA, Haldosen LA. Extracellular signal-regulated kinase (ERK) interacts with signal transducer and activator of transcription (STAT) 5a. Mol Endocrinol 1999;13:555–65.
[51] Yamaura M, Mitsushita J, Furuta S, Kiniwa Y, Ashida A, Goto Y, et al. NADPH oxidase 4 contributes to transformation phenotype of melanoma cells by regulating G2-M cell cycle progression. Cancer Res 2009;69:2647–54.
[52] Sturrock A, Huecksteadt TP, Norman K, Sanders K, Murphy TM, Chitano P, et al. Nox4 mediates TGF-beta1-induced retinoblastoma protein phosphorylation, proliferation, and hypertrophy in human airway smooth muscle cells. Am J Physiol Lung Cell Mol Physiol 2007;292:L1543–55.
[53] Crosas-Molist E, Bertran E, Sancho P, Lopez-Luque J, Fernando J, Sanchez A, et al. The NADPH oxidase NOX4 inhibits hepatocyte proliferation and liver cancer progression. Free Radic Biol Med 2014;69:338–47.
[54] Sherr CJ, Roberts JM. Living with or without cyclins and cyclin-dependent kinases. Genes Dev 2004;18:2699–711.
[55] Reiss K, Cheng W, Ferber A, Kajstura J, Li P, Li B, et al. Overexpression of insulin-like growth factor-1 in the heart is coupled with myocyte proliferation in transgenic mice. Proc Natl Acad Sci U S A 1996;93:8630–5.
[56] Meng D, Lv DD, Fang J. Insulin-like growth factor-I induces reactive oxygen species production and cell migration through Nox4 and Rac1 in vascular smooth muscle cells. Cardiovasc Res 2008;80:299–308.
[57] Qiao M, Shapiro P, Kumar R, Passaniti A. Insulin-like growth factor-1 regulates endogenous RUNX2 activity in endothelial cells through a phosphatidylinositol 3-kinase/ERK-dependent and Akt-independent signaling pathway. J Biol Chem 2004; 279:42709–18.
[58] Nakamura T, Colbert M, Krenz M, Molkentin JD, Hahn HS, Dorn II GW, et al. Mediating ERK 1/2 signaling rescues congenital heart defects in a mouse model of Noonan syndrome. J Clin Invest 2007;117:2123–32.
[59] Poolman RA, Li JM, Durand B, Brooks G. Altered expression of cell cycle proteins and prolonged duration of cardiac myocyte hyperplasia in p27KIP1 knockout mice. Circ Res 1999;85:117–27.
[60] Lloyd AC. The regulation of cell size. Cell 2013;154:1194–205.
[61] Hassink RJ, Pasumarthi KB, Nakajima H, Rubart M, Soonpaa MH, de la Riviere AB, et al. Cardiomyocyte cell cycle activation improves cardiac function after myocardial infarction. Cardiovasc Res 2008;78:18–25.
[62] Nakajima H, Nakajima HO, Dembowsky K, Pasumarthi KB, Field LJ. Cardiomyocyte cell cycle activation ameliorates fibrosis in the atrium. Circ Res 2006;98:141–8.
[63] Balasubramanyam K, Swaminathan V, Ranganathan A, Kundu TK. Small molecule modulators of histone acetyltransferase p300. J Biol Chem 2003;278:19134–40.
[64] Minucci S, Pelicci PG. Histone deacetylase inhibitors and the promise of epigenetic (and more) treatments for cancer. Nat Rev Cancer 2006;6:38–51.